



# Revolutionising orthopaedic implants—a comprehensive review on metal 3D printing with materials, design strategies, manufacturing technologies, and post-process machining advancements

Mustafiz Shaikh<sup>1</sup> · Fadi Kahwash<sup>1</sup> · Zhilun Lu<sup>2</sup> · Mohammad Alkhreisat<sup>3</sup> · Ashfaq Mohammad<sup>4</sup> · Islam Shyha<sup>1</sup>

Received: 3 April 2024 / Accepted: 29 July 2024  
© The Author(s) 2024

## Abstract

This paper conceptualises an understanding of advanced manufacturing methods to develop 3D-printed metallic orthopaedic implants, including a brief discussion on post-process machining. The significance of Metallic Additive Manufacturing (MAM) and its practicality for industrial applications is discussed through a juxtaposition with conventional casting and machining approach. Different alloys and suitable MAM techniques are thoroughly reviewed to determine optimum operating conditions. Although MAM can produce near-net shape parts, post-processing is an unavoidable requirement to improve surface quality and dimensional accuracy. A comparative study is presented, highlighting the importance of machining for post-processing in terms of cost savings and performance. Different materials are evaluated aiming to overcome problems associated with existing orthopaedic implants. The consequence of bone-implant mechanical mismatch leading to stress shielding and inadequate corrosion properties obstructing biodegradability are explored in detail. The effect of additive manufacturing parameters on mechanical, corrosion, and surface properties including biocompatibility is analysed. Evidence of MAM's advantages over conventional manufacturing approaches, such as the use of functionally graded lattices and patient-specific customised designs, is also presented. Finally, for future studies, a two-way approach is conceptualised with material selection and manufacturing process control in progressions of implant development using MAM.

**Keywords** Metal additive manufacturing · Orthopaedic implants · Stress shielding · Biodegradability · Post-process machining

## Abbreviations

MAM	Metal additive manufacturing	USFDA	United States Food and Drug Administration
3D	Three-dimensional	CE	Conformité Européenne
AM	Additive manufacturing	SLM	Selective laser melting
ASTM	American Society for Testing and Materials	EBM	Electron Beam Melting
ALVAL	Acute Lymphocytic Vasculitis Associated Lesion	MJT	Material jetting
		MEX	Material extrusion
		PBF	Powder bed fusion
		DED	Direct energy deposition
		BJAM	Binder Jet Additive Manufacturing
		CAD	Computer aided design
		TPMS	Triply Periodic Minimal Surface
		MRI	Magnetic Resonance Imaging
		CT	Computer Tomography

✉ Mustafiz Shaikh  
mustafiz.shaikh@napier.ac.uk

<sup>1</sup> School of Computing, Engineering and the Built Environment, Edinburgh Napier University, Edinburgh EH10 5DT, UK

<sup>2</sup> School of Chemical and Process Engineering, University of Leeds, Leeds LS2 9JT, UK

<sup>3</sup> Department of General Surgery and Special Surgery, Orthopaedic Department, Al-Balqa Applied University, As-Salt 19117, Jordan

<sup>4</sup> National Manufacturing Institute of Scotland, University of Strathclyde, Renfrew PA4 8DJ, UK

## 1 Introduction

The American Society for Testing and Materials (ASTM) defines Additive Manufacturing (AM) as a process which develops a product from a three-dimensional (3D) model by

joining or fusing the material in a layer-by-layer fashion [1]. Since its inception, 3D printing/AM has been used in rapid prototyping and repairing of engineering components. But recent development has made the process capable of developing parts used in automobile, defence, aerospace, electronics, and medical applications. Industries and researchers are attracted towards AM techniques as they present development of near net shape products with commercial profitability [2]. Most of the conventional processes require additional tooling such as cutters and dies. Moreover, traditional processes like machining inflate material wastage, which increases overall cost of these products. In additive manufacturing (AM), only specific feedstock materials are needed for production. In contrast, traditional machining requires a solid block of material, which is then shaped into the final part. This process is not sustainable and can increase overall cost. Through additive manufacturing, it is possible to achieve flexibility in design, ultimately resulting in fewer manufacturing stages required to make a component than its traditional counterparts [3]. Different manufacturing techniques have been assessed to design and develop 3D-printed orthopaedic implants. Based on the type of heat source and fusion technique, MAM is briefly classified as direct energy deposition (DED), powder bed fusion (PBF), material extrusion (MEX), and material jetting (MJT). Feedstock used in the process can be either a wire, powder, chips, or a foil [4]. Different techniques are still being developed and assessed for varied engineering applications. There are still concerns on using different metal alloys and composites which opens an area for studying MAM for functional relevance.

Metallic alloys are most prominently used for orthopaedic implants in knee/hip replacement, spinal fixations, and temporary fixators for fractured bones. Additionally, depending on the site and pathological diagnosis like osteoporosis, the implants mostly require metallic parts demanding high structural and fatigue strength [5]. But this high strength comes with a compromise. Materials such as stainless steel and cobalt-chromium alloy possess enough strength to be used for different orthopaedic applications, but they have very high Young's modulus compared to natural cortical bone causing stress shielding. This mismatch causes stress absorption by implants and passivation of supported bones, leading to an increase in osteoclastic bone degeneration cells, which results in reduced bone density [6]. With this continuous resorption, implant becomes less anchored to bone causing implant loosening. Titanium comparatively has lesser Young's modulus than other metallic alloys in the range of 100–120 GPa, but still the values are not closer to cortical bone. The Acute Lymphocytic Vasculitis Associated Lesion (ALVAL) is an inflammatory response associated with wear in metal-on-metal prosthetics, where elevated level in wear induced release of Cr and Co ions from implant

surface causes hypersensitive immune response and tissue damage [7]. Ceramic and polymer can be good replacement for metallic alloys, but the United States Food and Drug Administration (USFDA) does not recommend them for load-bearing applications. Ceramics have good wear resistance, but they are fragile with inferior ductility. Polymers on the other hand have shown pre-operative breakage and can also cause inflammatory reactions around the implanted area [8]. These restrictions could be subdued by development of porous metallic alloys with lower Young's modulus or ceramics with higher ductility.

The development of porous metal implants using AM technique is deemed possible which can reduce the impact of stress shielding. Arabnejad et al. [11] reported a reduction in stress shielding and its consequential bone resorption with development of 3D-printed porous titanium alloy. Their results were supported with a Digital Image Correlation (DIC) test and representative Finite Element (FE) model. Porous implants with optimised density presented reduction of 75% in bone resorption compared to conventionally manufactured fully dense titanium implant. Cronskär et al. [12] conducted a comparative study on commercial viability of AM for hip prosthesis. Seven implants were manufactured with conventional machining and Electron Beam Melting (EBM). Cost of production was compared by evaluating material price, design preparation period and overall manufacturing time. Considering these factors, the overall production cost of hip prosthesis with AM was 30% less than that of conventional machining process. Such studies prove the practicality of AM to develop orthopaedic implants. Figure 1 depicts multiple processing steps involved with conventional route in comparison to additive manufacturing of hip implant [13–15]. Table 1 represents a comparative analysis of improvement in characteristic properties of MAM-processed orthopaedic implants to traditional manufacturing approach; the data is theorised by summarising articles on manufacturing of orthopaedic implants [16–19].

## 2 Existing review status and current focus of study

We have conducted a thorough analysis to understand why it is important to revisit and evaluate popular subjects in MAM of orthopaedic implants. To perform this analysis of review status, the following methodical approach was considered.

1. Identify the topics being studied and under demand.
2. Map of significance, highlighting the trends.
3. Search of review article in the field of significance.
4. Identifying the need to collate with varied fields following a directed guide for future studies.

**Fig. 1** Processing steps involved in conventional route and additive manufacturing of a hip implant [9, 10]

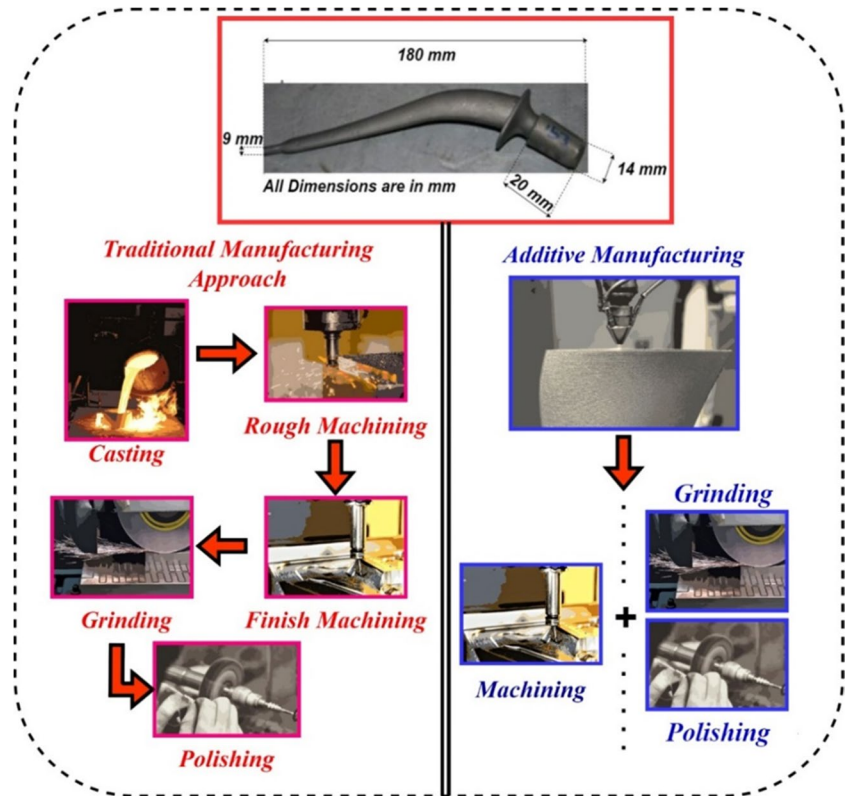


**Table 1** Comparison of effective improvement in functionality of MAM-processed orthopaedic implants in comparison to traditional manufacturing process

Characteristic property	Traditional process	Metal additive manufacturing	Improved properties
Precision and accuracy	Limited by machining possibilities	High precision with layer-by-layer control	Increased fit and functionality for complex shapes
Material utilisation	Significant waste in subtractive manufacturing	Minimal waste, near net shape production	Cost efficiency and sustainability
Complexity and design freedom	Restricted by tool access and machinist ability	Freedom to create complex organic shapes	Enhanced implant functionality with Improved patient outcomes and comfort
Customisation	Time-consuming and costly	Easy to produce patient-specific implants	Mimicking bone anatomy for improved fit and functionality
Mechanical properties	Dependent on bulk material properties	Tuneable through AM process parameters	Tailored strength, stiffness, and durability
Porosity control	Limited control over internal structures	Precise control over porosity and density	Better osseointegration and reduced stress shielding
Lead time	Long lead times for complex parts	Rapid prototyping and production	Faster time-to-market and patient treatment
Surface finish	Requires additional finishing processes	Can achieve high surface quality directly	Reduced need for post-processing
Biocompatibility	Standard biocompatible materials	Ability to use advanced, biocompatible alloys	Enhanced biological response and integration
Cost	High for custom and complex parts	Potentially lower for complex, customised parts	Lower overall costs with reduced waste and lead time

$$\text{Need}_{\text{Review}} = I[T, D] \rightarrow M_S \rightarrow R[S] \quad (1)$$

$\text{Need}_{\text{Review}}$  represents the need to perform the highlighted review.

$I[T, D]$  is the function that identifies important  $[T]$  topics based on their  $[D]$  demand levels.

$M_S$  is the function that creates a map of significance based on the identified important topics.

$R(S)$  is the function that searches for review articles based on the map of significance.

The process of first identifying key themes, then developing a map of significance, and lastly looking for review articles based on the map of significance is reflected in the theorised formula in Eq. (1). Throughout the investigation, we have looked for pertinent publications using Science Direct, Google Scholar, PubMed, IEEE Explore, Mendeley, ASME Digital Collection, and Web of Science. An analysis of research trends was conducted on the most recent studies spanning from 2018 to 2024.

Initially, we investigated subjects that would be of greater interest, using the keywords from the hot topics in metal additive manufacturing as presented in Fig. 2a. We have examined the present state of research in studies that use metal additive manufacturing to create a variety of orthopaedic implants. The following search terms were used to find relevant articles: biocompatible metal implant additive manufacturing, additive manufacturing in orthopaedic surgery, advances in 3D printing for orthopaedic devices, design, and process advancement in metal additive manufacturing of implants, and additive manufacturing of materials for orthopaedic implants. One hundred forty-eight publications were

examined, and VOSviewer™ was used to search for particular keywords and the study's focus. A network and heat map of the most popular subjects in demand since 2018 are shown in Fig. 2b. The most common keywords in this field were porous metals for bone scaffolding, patient-specific implants, stress shielding, topological and generative design, design-induced porosity, biodegradable implants, surface functionalisation, bone defect repair, bone tumour curing, aided healing, and bone ingrowth for osseointegration.

The heat map is used to display popular subjects in order of prominence. Following this examination, review papers relevant to hot subjects in AM of orthopaedic implants are evaluated and subsequently categorised into themes of the many topics under research. Figure 3 shows our examination of the review trend in MAM of orthopaedic implants. In total, 74 review articles were published over six years, with 54% concentrating on material analysis, 12% on general themes, and 8% each on manufacturing, design, post-processing, and application. The need to conceptualise, a collated understanding of material, manufacturing, design, application, and post-processing of additively manufactured orthopaedic implants arises from noticing the trend. Therefore, this paper attempts to bridge this gap by providing a comprehensive analysis with primal additional focus on stress shielding and biodegradability concepts in orthopaedic implants, which are crucial in defining the functionality of both temporary and permanent devices. Figure 4 illustrates various orthopaedic devices and the importance of addressing issues related to stress shielding and degradation in these implants.

Stress shielding occurs in implants made of high-strength materials with greater elasticity than cortical bone, leading

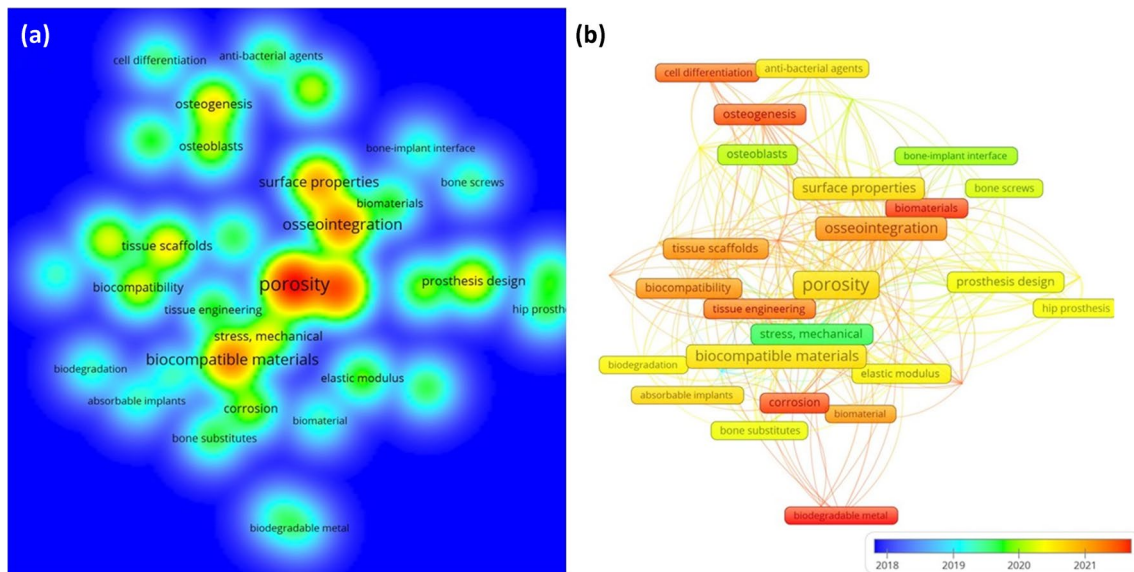


**Fig. 2** Hot topics in metal additive manufacturing of orthopaedic implants between 2018 and 2024. **a** Significant and **b** connected keywords

**Fig. 3** Review trend in 6 years for MAM of orthopaedic implants in 74 review articles

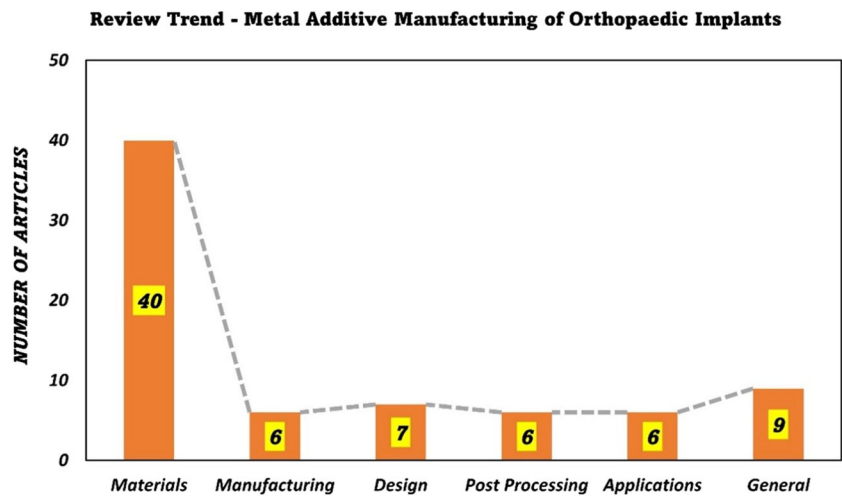
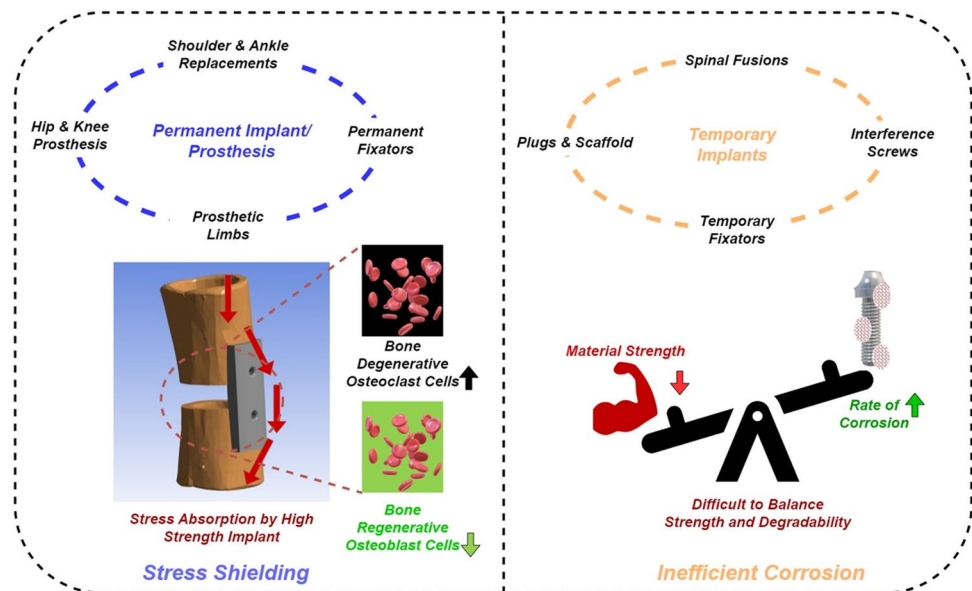


**Fig. 4** Problem associated with stress shielding and bioabsorption in orthopaedic implants



to the immobilisation of bone supported by these implants. Natural bone growth relies on osteoclasts and osteoblasts cells, responsible for bone degeneration and growth respectively [20, 21]. The immobilisation caused by stiff implants inhibits the natural bone growth process, leading to increased osteoclast activity and reduced bone density. This can result in implant loosening, infections, the need for revision surgery, and additional complications [21].

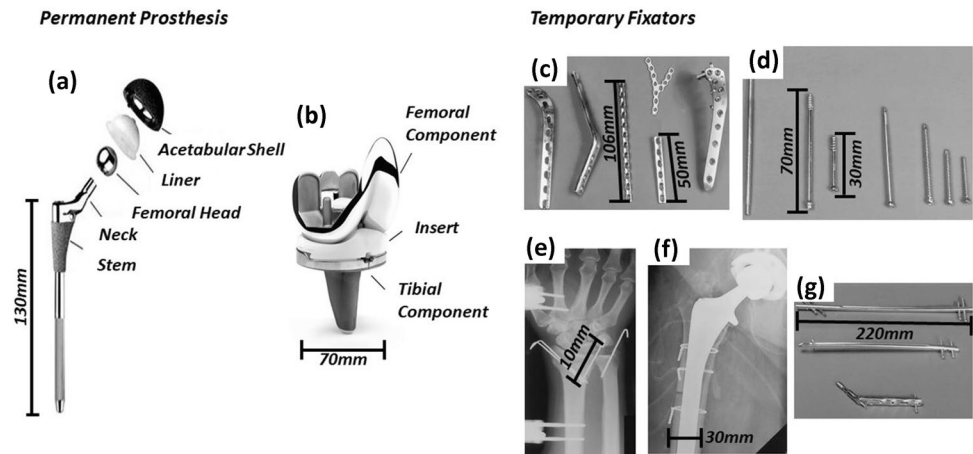
Conversely, achieving a controlled rate of degradation is crucial for temporary implants to avoid the economic, staffing, and patient burdens associated with surgical removal post-bone healing [22]. A major challenge in developing absorbable implants is striking a balance between achieving the desired corrosion rate and maintaining sufficient structural strength [23]. Additively manufactured metallic devices show promise in achieving this balance [24].

This review presents insights into resolving stress shielding and biodegradation through metal additive manufacturing, which was missing in available literature. In addition to discussing material selection, design methodologies, process control during manufacturing, and post-processing capabilities, the review also proposes a roadmap for researchers to systematically develop orthopaedic devices with defined materials and manufacturing approach.

### 3 Orthopaedic implants

Orthopaedic devices are briefly classified as permanent and temporary implants. Figure 5 shows the classification of implants in current clinical use. Apart from hip, and knee replacement as signified in Fig. 5, with current technological

**Fig. 5** Classification of orthopaedic implants: **A** hip prosthesis, **B** knee prosthesis, **C** fixation plates, **D** screws, **E** pins, **F** wires, and **G** intramedullary rod [25]



advancements, development of shoulder, ankle, wrist, and finger joints have been possible [25]. Artificial joints and prosthesis fulfilling the need of a damaged or deceased bone are termed as permanent implants. They tend to remain in patient's body for their whole lifespan. The need for orthopaedic implants and devices is also increasing due to growth of global ageing population [26]. Upsurge in obesity and injuries related to sports are also a major reason. Increasing elderly population require a total hip or knee replacement to support healthy lifestyle. Farrow [27] predicts the requirement of hip arthroplasty in Scotland to increase by 27% in 2038. Avascular Necrosis, Arthritis and Osteogenesis are some bone diseases contributing to growing demand for joint replacements in young and middle-aged population [28]. Rise in demand for joint replacement is a major concern in the United States; more than 50% of joint replacement patients are under the age of 65 [29]. In general, the need and demand for permanent implants is increasing and is not a factor depending on age.

Temporary fixators are the other classification of orthopaedic implants with rising demand. They are used to support and fix distorted or fractured bone. Screw, pins, plates, and wire are used to hold fragmented and deformed bones. Where fractured long bones are held using an intramedullary rod. These implants in some cases are required to be removed surgically on completion of bone healing period of usually 4–16 weeks [30]. Existing trends point towards the

development of bio-degradable fixators. Materials that have very high Young's modulus are currently used which require a revision surgery to remove fixator after the bone healing period. ActivaPin™ is a poly(l-lactide)-co-glycolic acid (PLGA) bioabsorbable implant produced by Bioretec®, used in clinical practice to fix hammer toe fractures. But implementation of degradable polymers for other fixation implants is yet uncertain, as they have low load-bearing strength [31]. Researchers are also working on developing magnesium and calcium-based bio-degradable bone and spinal fixators. MAGNEZIX®(Mg-Y-RE-Zr) are European Conformity (CE) approved magnesium alloy currently in human trial used as absorbable screws in spine and elbow fracture [32]. Different metallic materials are still under study, accessed to be used as biodegradable orthopaedic implants.

#### 4 Orthopaedic implants—materials for additive manufacturing

Stainless steel, titanium, and cobalt chromium alloys are most widely used metallic materials for orthopaedic implants. Polymers and ceramics have also been under study. Considering the significant concerns of stress shielding in permanent implants and biodegradability in temporary implants, MAM is an emerging and highly relevant technology currently employed to address these issues. USFDA is a

**Table 2** USFDA approved metals for orthopaedic implant application [34]

Metal implant type	Clinical application	Implant duration	FDA cleared alloys/metals
Bone fixation	Plates, screws, wires, pins, and rods	Temporary/permanent	Titanium, stainless steel, nickel-titanium, silver, gold, platinum
Prosthesis	Hip prosthesis, knee replacement	Permanent	Titanium, cobalt-chromium, stainless steel, nickel alloys

global regulatory body which follows a stringent process of evaluating materials for medical device applications. They have published list of approved metallic materials used for orthopaedic implants and devices. Table 2 presents list of materials currently in use and their application (last updated in July 2024). Apart from the following list of approved materials, FDA also suggests the use of magnesium alloys, but its approval is still subject to long term human trial studies [33].

#### 4.1 Permanent implant materials

SS316 stainless steel is used for both fracture fixation and permanent prosthesis. Although they have been in use for a long period, recent studies show that these metallic alloys release Ni and Cr which are toxic and can cause dermatitis skin infection. American Society of Testing Materials (ASTM) recommends the use of SS316L due its lower composition of carbon resulting in lower overall stiffness [35]. Titanium and its alloys are another group of metallic materials, where Ti-6Al-4V is well established for use in dental and orthopaedic applications. Even this class of metallic alloys are considered cyto-toxic as they release Al and V in long implantation which can cause serious illness like Alzheimer's disease [36]. Development of Ti-15Zr-4Nb-4Ta alloy resulted in comparatively less toxicity.

Chromium cobalt alloys particularly Co-28Cr-6Mo and Co-26Cr-6Mo-0.2C have been in use for knee replacements prosthesis. Reports on additive manufacturing of these materials prove development of similar alloy composition with lower ultimate tensile strength and reduced percentage of fracture elongation, contributing to reduced stress shielding [37]. Tantalum (Ta) alloys have self-passivating capacity, where the ions procreate forming an anti-corrosive barrier to body fluids. But the applications of Ta are limited due to their high manufacturing cost associated to their high melting point of 3017 °C [38]. Although traditional metallic alloys possess high stiffness and strength contributing to stress shielding, they possess excellent corrosion and wear resistance which are significant for biocompatibility [39]. The development of porous class of these metals using additive manufacturing can invariably reduce stress shielding effect. These classes of porous implants are considerably better than polymeric materials like PEEK and highly brittle calcium phosphate ceramics, since they can be ineffective in terms of either being toxic or brittle. Therefore, this review emphasises on studying manufacturability of metal alloys for orthopaedic applications. Reports on developing components from 316L stainless steel, Ti-15Zr-4Nb-4Ta, and Co-26Cr-6Mo-0.2C using electron and laser-based additive manufacturing techniques are now available in the literature [40, 41].

Zirconium metal and its alloys have been used for total hip and knee arthroplasty applications [42]. They are also reported on being utilised as osteosynthesis plates for diaphyseal fractures. Alloying or coating of zirconium oxide with titanium and stainless steel are correspondingly employed as they possess excellent corrosion resistance [43]. Although zirconium shows higher significance for being used as orthopaedic implants, its development with additive manufacturing is limited due to its pyrophoric property and high reactive nature [44]. However, direct energy deposition technique has been employed to use zirconium as coating over titanium and cobalt chromium alloys effectively improving their biomechanical properties [45].

#### 4.2 Temporary implant materials

Temporary implants are used for a particular period and then removed after bone healing through revision surgery, which is inconvenient for patient and surgeon alike. USFDA has approved polymeric and ceramic materials only for non-load-bearing applications for screws, nails, and pins. Metallic components such as magnesium, zinc, and iron with the alloys of calcium, strontium and ytterbium are being studied to be implemented for compressive applications [46]. CE has approved some class of magnesium alloys for biodegradable implant application, where MAGNEZIX® implant is a prime example.

Magnesium alloys are gaining tremendous interest since they are non-toxic, and their mechanical strength is comparable to natural cortical bone. High corrosive property is the major hinderance which limits the use of Mg for high strength orthopaedic applications. Coating and alloying of Mg with different materials have however resulted in improvement of its degradation property [47]. These alloys and composites find application in temporary implants for bone plates, screws, and cardiovascular stents. Powder bed fusion technique of laser beam melting has been employed to additively manufacture Mg alloys [48]. Esmaily et al. [49] conducted a study on additive manufacturing of WE43 Mg alloy using SLM technique, where influence of zirconium oxide in the alloy microstructure and non-uniform composition resulted in higher rate of corrosion. They suggested to conduct a study to further understand and control the powder characteristics wherewith corrosion resistance could be improved.

Iron and its alloys have also been in use for temporary implant applications, but their degradation rate is slower compared to bone healing period. Different approaches have been attempted ranging from alloying and coating to suitably control their bio absorption. Wegener et al. [50] conducted an experiment to study osteo compatibility of porous iron-based implant. Studies revealed new bone growth in cellular spaces with sign of brief implant degradation. Further

studies on iron-based open cellular biomaterials for high load-bearing temporary implant devices were suggested. Li et al. [51] reported the first ever additive manufacturing of functionally graded topologically designed porous iron for biodegradable implant application. These porous implants presented 5–16% weight loss in 4 weeks, which is below the required range for bone substitution. Zinc is another class of metallic material used as a biodegradable implant. Corrosive property of it lies between Mg and Fe. Their degradation rates are higher than those of Mg and lower than Fe, making them suitable material for temporary implant applications [52]. However, the daily safe dose of Zn in human body is much lower than that Mg, making them a good alternative only for small devices [53]. Additively manufactured Zn are extremely mushy and porous since they have low melting point and vaporisation temperature. Demir et al. [54] proposed the use of open chamber selective laser melting with inert gas jet flow over powder base to develop Zn parts with over 99% density.

Table 3 lists different metals currently being investigated and corresponding MAM technique used to manufacture the orthopaedic implants. 316L SS, Ti, and Co-Cr alloys are mostly investigated for permanent prosthesis as they present high mechanical strength and sufficient wear resistance for long term use in joint implants, although ceramics implants are considered the best alternative where high wear resistance is required, where Fe, Mg and Zn are studied for temporary applications as they are soft materials susceptible to degradation. Although these materials show improved characteristics, the problem of mechanical mismatch between metallic alloy and cortical bone for permanent implant and controlled degradability for load-bearing application in temporary implant is still not solved. This opens an area of study to further optimise and analyse MAM for suitability of diversified implant application for clinical use. Table 4 represents different materials including polymer, ceramic, and metals with their comparative properties to Bone's elastic modulus and yield strength. A comparison of conventionally (CM) and additively (AM) manufactured metal is also presented.

## 5 Orthopaedic implants—metal additive manufacturing techniques

Powder bed fusion (PBF), direct energy deposition (DED), material extrusion (MEX), and material jetting (MJT) are broadly categorised metal AM techniques used for implant manufacturing. Figure 6 represents schematics of these process with their advantages and shortcomings. PBF is divided into selective laser melting (SLM) and electron beam melting (EBM) based on the energy source. SLM uses a laser to melt metal powder in an inert gas atmosphere, where

producing amorphous metals is its unique advantage with faster cooling. However, issues like cracks and high residual stress in SLM led to the development of EBM. Introduced by Arcam in 1997, EBM uses an electron beam in a vacuum chamber, reducing oxidation and producing denser parts. Despite higher manufacturing costs and limitations with certain materials, EBM is very popular with its significant advantages in achieving minimised residual stress and process-induced defects like cracks.

DED involves simultaneous melting and deposition of metal powder using a laser or electron beam. It is efficient for large build volumes and is very beneficial for coating and repairs. Binder Jet Additive Manufacturing (BJAM), developed by MIT and commercialised in 2010, uses a powdered base material and a liquid binder. BJAM allows faster printing without support structures and uses coarse powders, reducing costs. However, products require extensive post-processing, including sintering, to address shrinkage and porosity, limiting their suitability for intricate engineering applications.

Each technique has unique advantages pertaining to their process parameters, influencing their application in implant manufacturing. Table 5 represents specific process parameters for these techniques and their relevant significance.

PBF is the commonly used 3D printing technique, since its highly manageable and parts produced through this process have comparably better properties to their conventional counterpart. More reports are published with use of SLM since it provides better geometrical tolerance compared with EBM, and better structural properties compared to BJAM. Lewin et al. [119] compared additive manufacturing performance of titanium mesh produced by EBM and SLM with  $\mu$ CT analysis. Their study revealed a 13–35% deviation in a cross-sectional area to design geometry for EBM produced part, where the range of deviation exhibited by SLM parts were below 2%. Figure 7 represents dimensional accuracy of SLM over EBM.

Although EBM has difficulty in processing with higher dimensional accuracy, their parts possess less residual stress, higher strength, and lower contamination by gasses in final product, which is a major advantage considering the production of orthopaedic implants. Considering their exceptional processibility, studies examining the geometrical characteristics of EBM produced parts to improve and optimise them is of utmost importance. Béraud et al. [120] conducted a study to improve dimensional accuracy for small parts produced by EBM. They conducted a simulation displaying dependence of beam diameter on focus current. Further optimisation of beam trajectory resulted in reduction of manufactured and nominal diameter difference to 61.2%. More studies on optimising and improving dimensional accuracy will facilitate in increasing process capability of EBM for smaller parts.

**Table 3** Reports on MAM of orthopaedic implants

Material	Application	Significance and drawback	Reported MAM technique	References
Stainless steel	Locking fixation system, and orthodontic devices	↑ Mechanical strength, suitable for prosthesis, release of Ni, Cr cause dermatitis skin infection, SS316L—good biocompatibility and stiffness ↓	SLM, DED, EBM	[55–59]
Titanium	Cranial implants, scaffolds, trabecular components, knee, and hip arthroplasty	Reduced stress shielding with ↓ Young's modulus, Ti–Al–V cytotoxic with release of Al and V, Ti–Zr–Nb–Ta—↓ toxicity	SLM, DED, EBM	[60–66]
Co-Cr	Metaphyseal femur fixation, knee and hip arthroplasty, and scaffolds	↑ Manufacturability, reduced stress shielding, ↑ imaging capability for post-operative imaging	SLM, DED, EBM, and laser energy net shaping	[67–71]
Tantalum	Bone grafts, spinal implant, acetabular cups	↑ Osseointegration, excellent corrosion resistance, biocompatibility, ↑ porosity for bone ingrowth	SLM, EBM, direct metal laser sintering	[72–74]
Zirconium	Hip and knee replacements, orthodontics	↑ Biocompatibility, excellent corrosion resistance, ↑ mechanical properties, stable oxide layer	SLM, EBM	[75–78]
Magnesium	Biodegradable implants, screws, pins, plates, and scaffolds	Non-toxic, supports bone growth, but ↑ corrosion	SLM, DED, EBM, B/AM	[79–83]
Zinc	Scaffolds and cardiovascular stents	Corrosion rate between Mg and Fe, but not manufacturable with ↓ melting point and vaporising temperature	SLM, DED, EBM	[54, 84–87]
Iron	Intramedullary nails, bioresorbable implants, and scaffolds	Supports haemostasis, biocompatible, but ↓ corrosion	SLM, DED, EBM	[88–93]

**Table 4** Material properties of metals in comparison to bone, ceramic, and polymer

Material	Elastic modulus (GPa)	Tensile strength (MPa)	References
Bone	10–30	50–150	[94]
Ceramic—alumina	415	665	[95]
Polymer—PEEK	3.95	103	[96]
Stainless steel—AM	150–180	500–1100	[97]
Stainless Steel—CM	190–210	520–1100	[98]
Titanium—AM	90–110	700–950	[99]
Titanium—CM	100–120	900–1000	[100]
Co-Cr—AM	210–220	800–1200	[101]
Co-Cr—CM	220–230	900–1300	[102]
Tantalum—AM	185–200	200–400	[103]
Tantalum—CM	190–210	300–500	[104]
Zirconium—AM	88–100	330–700	[105]
Zirconium—CM	100–110	500–900	[106]
Magnesium—AM	40–45	150–250	[107]
Magnesium—CM	45–50	200–300	[108]
Zinc—AM	70–100	100–200	[109]
Zinc—CM	100–110	500–900	[110]
Iron—AM	200–210	200–350	[111]
Iron—CM	210–220	250–400	[112]

### 5.1 Manufacturing and design developments

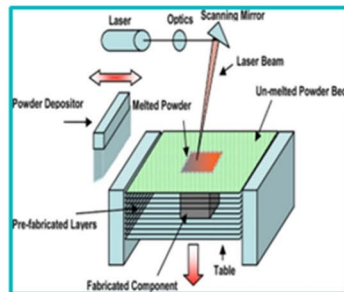
Orthopaedic implants vary in shape and design depending on end application. Topology and porosity vary in accordance with the specific requirements. Cortical bone implants, which are intended to carry and support function of a dense bone, require parts with high strength, in the order of 90–209 MPa, whereas cancellous or trabecular bone implants used as scaffolds are required to be porous with comparatively lower strength in the range of 1.5–45 MPa [121]. Different bone structures in a femur can be seen in Fig. 8.

MAM facilitates the development of metallic parts with a wide range of porosity, mimicking original bone structures. Conventional and other advanced manufacturing methods like liquid state processing, powder metallurgy, electron and vapour deposition can produce porous metallic parts, but range and order of pores are completely random. Although the percentage of porosity can be controlled to some extent, the geometry of pores is mostly irregular. With topological optimisation of MAM, pores with predefined external shape and internal architecture can be designed [123]. As seen in Fig. 8, realisation of parts with graded pores mimicking (a) head, (b) neck, and (c) metaphysis structures is possible with MAM.

## Metal Additive Manufacturing

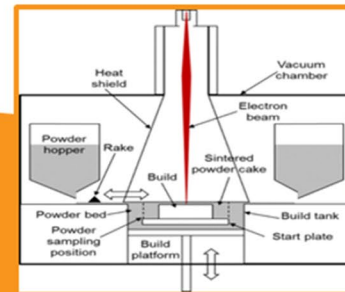
### Selective Laser Melting

- LASER used to melt powder in Inert Atmosphere
- *Good Geometric Resolution*
- *High Residual Stress*



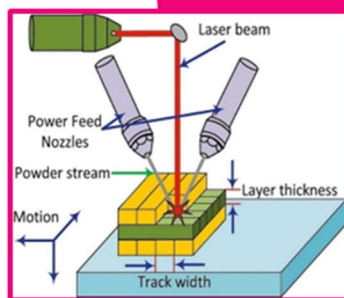
### Electron Beam Melting

- Electron Beam Melts powder in Vacuum Atmosphere
- *Less Contamination*
- *Volatile for low melting point metals*



### Direct Energy Deposition

- Powder melted and deposited with Laser/Electron Beam
- *Faster Build*
- *Low Geometric Resolution*
- *High Surface Roughness*



### Binder Jetting

- Binder adhesive employed to fuse metal powder
- *Multi-material, Complex shapes processing*
- *2 Stage Process, requiring curing of binder*

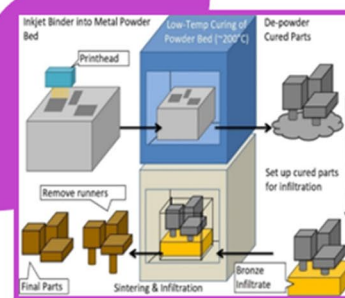


**Fig. 6** Metal additive manufacturing techniques with their significant advantages and shortcomings [113–116]

**Table 5** Different MAM techniques used for orthopaedic implants with their unique significance [117, 118]

MAM technique	Process parameters	Significance
Selective laser melting	Layer thickness ( $t$ ), laser power ( $P_L$ ), scan speed ( $V_S$ ), Hatch distance ( $d$ ), and scan strategy	<ul style="list-style-type: none"> <li>Higher cooling rates lead to smaller grain sizes, increasing strength</li> <li>Amorphous metals can be developed with low beam diameter, high scanning speed, and high beam power</li> </ul>
Electron beam melting	Layer thickness ( $t$ ), scan speed ( $V_S$ ), Hatch distance ( $d$ ), scan strategy, beam focus, beam power ( $P_E$ ), beam velocity, and beam diameter	<ul style="list-style-type: none"> <li>Ideal for manufacturing brittle alloys with reduced residual stress</li> <li>High energy beam allows for larger layer thickness and faster processing</li> </ul>
Direct Energy Deposition	(A) Laser beam Layer thickness ( $P_S$ ), laser power ( $P_L$ ), scan speed ( $V_S$ ), Hatch distance, scan strategy (B) Electron beam Beam focus, beam power, beam velocity, beam diameter	<ul style="list-style-type: none"> <li>Functionally graded material processing is possible</li> <li>Enables simultaneous printing and surface defect repairs</li> </ul>
Binder Jet Additive Manufacturing	(A) MAM Layer thickness ( $t$ ), binder saturation, roller traverse speed (B) Sintering Cycle time and temperature	<ul style="list-style-type: none"> <li>Not limited by material properties, any materials can be combined and printed</li> <li>High powder recyclability with no heat involved in printing stage</li> <li>Heating only in curing/sintering stage, minimizing heat-induced stress</li> </ul>

**Fig. 7** Geometrical variance observed in parts processed through EBM and SLM **a** cross section area comparison of laser (blue) and electron (green) beam processed parts with cad geometry (black), **b** electron beam processed part in comparison to **c** laser beam for tensile specimen, and **d** cranial implant geometry under study [119]

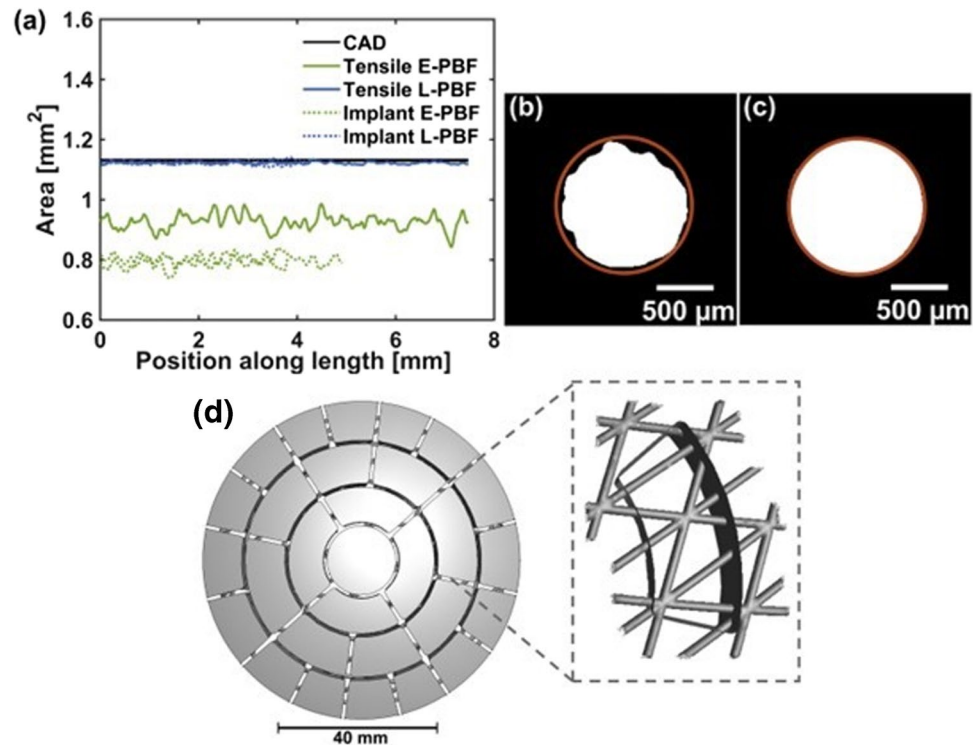
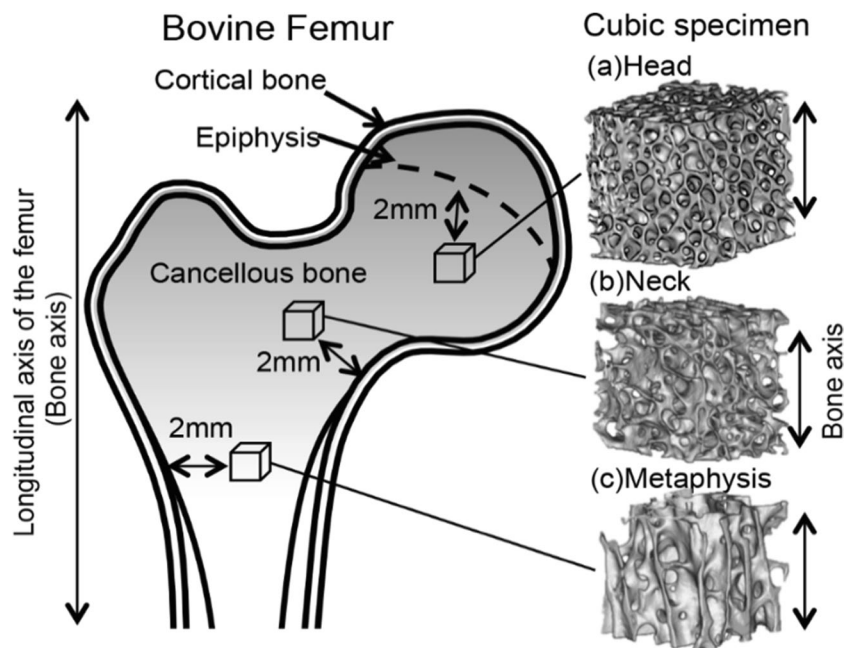


**Fig. 8** Femur bone with differential **a** head, **b** neck, and **c** metaphysis structures [122]



Topological optimisation is a design strategy, where geometrical structure and features are graded with relevance to user specific requirement. Finite Element Method (FEM) is currently employed to topologically optimise the design in accordance with suitable structural and mechanical property necessities. This technique has been implemented to develop improved implant designs for both porous and non-porous applications.

Carnicero et al. [124] performed a topological optimisation for additive manufacturing of Ti-6Al-4 V subperiosteal maxillary atrophy implant. They analysed implant design with 2-phase FEM based topological optimisation. FEA analysis was performed on implant's geometry considering loading cases for critical and standard chewing forces; additionally, effects of fastening conditions were also studied. This simulation was used to critically analyse portions

of implants that could be altered, attaining a modified new lower volume part. Designs developed through this process resulted in 28% volumetric reduction and eliminated the requirement of two fastening screws. The study also showed the optimised designs performing well under tensile-compressive and fatigue conditions. This flexible design strategy led to successfully manufacturing of implants with better properties and less production cost, made possible through MAM.

Considering the capability of MAM in manufacturing complex designs, TPMS (Triply Periodic Minimal Surface) are gaining significant attention. These designs offer a unique combination of high strength, lightweight structure, and large surface area, which are essential for implants. TPMS structures can be precisely tailored to match the mechanical properties of natural bone, thereby reducing stress shielding and

promoting better integration with the biological tissue. Additionally, the porous nature of TPMS designs enhances osseointegration and vascularization, improving the overall success rate of orthopaedic implants. This innovative approach in MAM allows for customised, patient-specific solutions, significantly advancing the field of medical implants.

In TPMS designs, one open cellular unit cell of minimal surface design is used in a continuous repeated order to form a porous part. Gyroid, Schwarz, Neovius, and D-Prime are four major types of TPMS architecture. Amongst the different designs, network solid gyroid structure is most suitable for biomimicry of orthopaedic implants. These structures have interconnected pores and provide better control of pore volume fraction [125]. Mathmod is a computer software which supports visualisation and manipulation of different TPMS models by mathematical equation.

$$\text{Gyroid surface} : F(x, y, z) = \cos(x) \cdot \sin(y) + \cos(y) \cdot \sin(z) + \cos(z) \cdot \sin(x) + \alpha \quad (2)$$

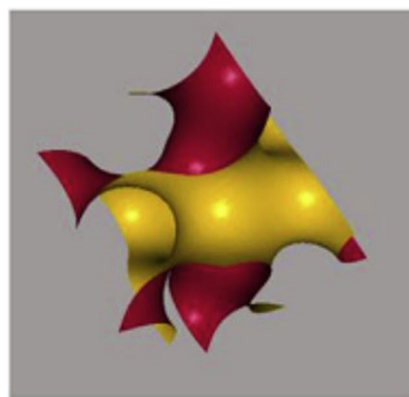
Equation (2) represents a simple gyroid unit cell [126], where  $\alpha$  is an iso function which controls the porosity in the TPMS. Higher  $\alpha$  values result in larger pore diameter and distance between gyroid surfaces [127].  $x, y, z$  are the cartesian coordinates of surface points. The upper and lower limits of the coordinates are dictated by the required size of the TPMS cell. For example, for a sphere of radius 4,  $x, y$  and  $z$  can be between  $-4$  and  $4$ .

Figure 9a shows the gyroid unit cell designed with Mathmod, and Fig. 9b shows a  $9 \times 6 \times 12$ -mm block of scaffold designed with 3-mm network gyroid structure. Mechanical analysis of additively manufactured TPMS parts shows improved fatigue property due to curvature of struts, and at nodal points, stress concentration caused by defects is also reduced. TPMS-based parts have proven to provide better chances to inherit biomimicry with possibility of designing intricate porous architecture [129]. Yan et al. [130] analysed manufacturability of TPMS design using Ti-6Al-4 V with

SLM. They developed samples having 80 to 95% of porosity which showed experimental elastic modulus in the range of 0.15 to 1.3 GPa. Where their prediction with regression model presents capability to produce TPMS design using Ti with 5 to 10% porosity having elastic modulus closer to cortical bone, which can be used for load-bearing implants without inducing any stress shielding effect.

One of the major advantages of MAM is possibility of producing patient-specific implant. Images obtained through Magnetic Resonance Imaging (MRI) and Computer Tomography (CT) can be used as a 3D model for additive manufacturing. Implants produced by this technique can be of exact fit and dimension suitable for a particular patient [131]. OsiriX imaging, 3D Slicer, Mimics, and In Vesalius are software packages which have been used earlier to convert a CT/MRI image into 3D model suitable for additive manufacturing [132]. Edelmann et al. [133] presented the potential of developing patient specific osteosynthesis implant using SLM.

**Fig. 9 a, b** Gyroid and TPMS designed scaffold [128]



**(a) Typical Gyroid Structure (b) TPMS Architecture Scaffold**

These implants displayed high fitting accuracy and sufficient mechanical properties suitable for orthopaedic application. The development of such customised implants can lead to the elimination of pre-operative procedure like bending, cutting, or shape trimming of conventionally designed bone plates. Production of these personalised implant followed a five-stage process of Image acquisition using CT, image segmentation, Standard Tessellation Language (STL) file processing, CAD construction, and additive manufacturing.

Figure 10 represents digital process plan followed to physical realisation and additive manufacturing of customised osteosynthesis implants. Initially CT scan of tarsal feet fracture was used for image acquisition. In Vesalius provided segmentation and conversion of CT image to a 3D model. Autodesk Meshmixer aided in developing a defined 3D model with closed open surface area. CAD file suitable for additive manufacturing was finally developed using Autodesk Enabler. These intricately followed step by step multi software, digital to physical process chain enabled development of patient specific additive manufacturing of osteosynthesis implants.

## 6 Post-processing of orthopaedic implants

Powder bed fusion additive manufacturing can successfully develop near net shape implant devices. But the surface finish is often substandard requiring additional post-processing. Depending on application, implants require different grade of surface finish. Surface properties like microstructure, roughness, and topography play a vital role in

biocompatibility of implanted devices. Osseointegration is a four-stage biological process defining cell surface integration of bone-implant interface. Soon after the surgery, bone and implant gap are filled by coagulated blood. This blood coagulation further recruits phagocytic or white blood cells to remove necrotic or dead tissues. They also attract new multipotent mesenchymal cells, which migrate to implant surface resulting in osteo conduction, forming a thin layer of bone cells. Less than 1 mm of minimal distance between implant and host bone surface is required to provide proper anchorage. The thin layer of mesenchymal cells further differentiates into osteoblast which result in woven bone formation after 4 to 6 weeks. These woven bones later get replaced by more mature and structurally strong lamellar bone. Optimal osseointegration is a function of material and surface property of an implant [134].

Highly polished fine finish is required for temporary implants like plate and screws and permanent implants like hip and knee prosthesis, where friction can induce corrosion and metallic wear. On the other hand, scaffolds are needed to possess rough surface to initiate and support bone ingrowth. Different applications require varying medium of post-processing. Figure 11 represents requirement of surface roughness values for different types of implants. Acetabular cup and femoral head components of a total hip prosthesis are in regular contact inducing friction causing material debris due to wear. ISO 7206–2 suggests surface characterisation and maximum allowance of surface roughness for optimal success of Total Hip Arthroplasty (THA). Recommended average roughness ( $R_a$ ) value for femoral head component is  $0.05 \mu\text{m}$ , where for acetabular liner it is to be under  $2 \mu\text{m}$  [135].

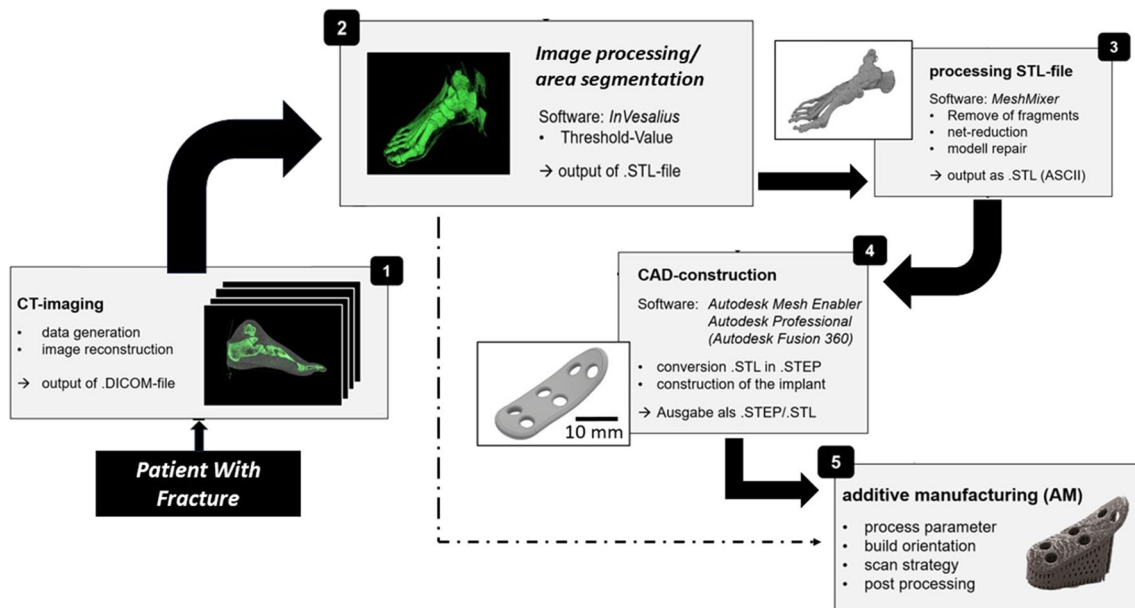


Fig. 10 Digital to physical process chain for MAM of patient specific implant [133]

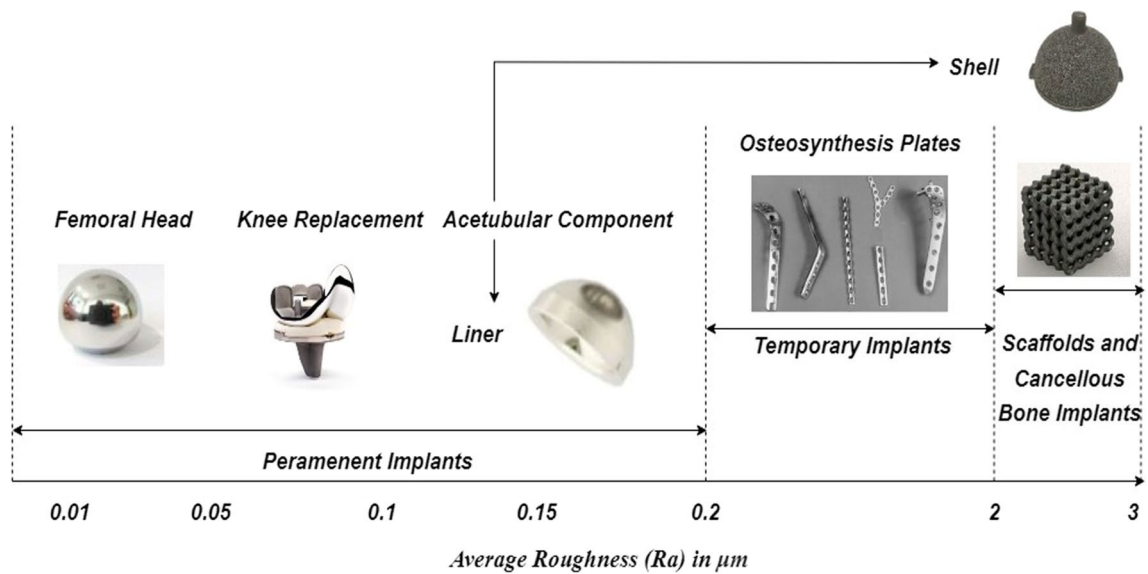


Fig. 11 Roughness requirements for osseointegration of different implant [137–139]

Hayes and Richards [136] postulated a hypothesis recommending temporary implant to possess  $R_a$  in the range of 0.2 to 2  $\mu\text{m}$  for achieving optimal osseointegration. These implants are either required to be biodegraded or removed with revision surgery upon completion of bone healing period. They conducted an in vitro analysis of their hypothesis, with microrough and smooth surface fracture fixation implants. Temporary implants with smooth surface avoid bone overgrowth facilitating easy biodegradation and implant removal, whereas rough surface fixators increased bone contact, adding difficulty in implant removal and complete degradation. Fracture fixation devices in contrary to permanent implants do not require complete osseointegration. Therefore, in accordance with the experimental validation, the hypothesised range of roughness parameter is well suited for successful implantation of screws and plates for osteosynthesis application.

### 6.1 Available methods in surface post-processing of MAM parts

Techniques ranging from sand blasting, grinding, abrasive/electropolishing, and finish machining have been implemented for surface post-processing of orthopaedic implants. Inherent aim of these techniques is to improve materials' aesthetics, wettability, and corrosive properties. In MAM, this is achieved by following a sequential order. Initially support structures are removed, followed by removal of excessive powders. Additional features are needed to be developed if required. Surface finish is the most important step as 3D-printed materials have very rough surface of order  $7 \pm 1 \mu\text{m}$  [140]. Further coating is also applied in accordance

with the requirement. Post-processing technologies are broadly categorised into two groups, namely mechanical and chemical methods.

Mechanical methods include grinding, lapping, polishing, sand blasting, and machining. Grinding, lapping, and polishing can develop parts with very low surface roughness, where machining has a capability of improving surface quality and developing additional features when required. Chemical methods such as coating, electropolishing and etching must be selected by considering their end effects on material biocompatibility, as the reaction can induce formation of surface level toxic layer.

Surface texture and topography are analysed to characterise the surface properties. Roughness, waviness, lays, and flaws are measurable characteristics used to analyse the surface quality. Roughness is a measure of vertical deviation from primal surface, where  $R_a$  and  $R_z$  are numerical parameters used to represent their average degree of difference. These amplitude parameters are most common measure used for studying surface topography of orthopaedic implant [141]. Surface waviness is horizontal measure of spacing between adjacent local peaks; these irregularities are formed due to work-piece deflection, improper damping causing vibrations, and heat treatment effects. Lays are directional surface textures formed due to the nature of manufacturing process. Flaws are cracks, scratches and inclusions effecting properties like corrosion and fatigue. Surface topography and texture are function of material characteristics and nature of process. They vary in accordance with the initial and post-manufacturing process. Mechanical stylus, optical interferometry, and microscopy are three characterisation techniques used to measure surface properties.

Teo et al. [142] characterised surface properties on different post-processing methods of additively manufactured Cellular Metallic Material (CMM) 316L stainless steel for biomedical application. CMM are porous parts with well-defined architecture of pores formed by repetitive unit cell. A sequential process starting from sand blasting, abrasive polishing, to electropolishing was conducted to effectively improve surface properties of internal and external features of the CMM part. The as-printed part revealed partially molten particles causing high surface roughness. Figure 12 shows findings from each post-processing methods of Teo's study. A need for further study is required to improve post-processing strategy for additively manufactured CMM parts having better surface roughness with less surface defects. Moreover, the presented strategy is not time or cost effective. A need for single step post-processing method capable of improving surface quality is emphasised by this study for economic feasibility.

## 6.2 Why machining post-MAM?

Post-processing studies on MAM is still in early stage of investigation, with varied available options. Mechanical machining has overhand to other techniques in terms of being a well mature process involving decades of research providing ability to optimise the process for achieving target surface and bulk properties. Problems discussed in the previous section such as peel off layer, pits, and microcracks can be managed with machining in a single process making it an efficient choice. Figure 13 in overall represents how a clean defect free surface is achievable with surface milling, also representing cost economics proving financial benefit

of using machining as post-processing technique for MAM parts. Figure 13a represents rough surface with irregular topography of a MAM part, where a clean surface with possibly lowered surface defects can be obtained with machining. Although some surface marks and micropits are still visible in Fig. 13b, they can still be managed by optimising machining process parameters, and moreover, more severe surface defects like peel off layer, larger pits, and cracks are eliminated by a single process in machining proving its efficiency over other post-processing methods.

Maleki et al. [143] compared different material and non-material removal based mechanical, and laser techniques with coating and hybrid processes. A comparative study was conducted with a cost analysis matrix having time and money as the key factor each with a score from 1 to 5. Each treatment was ranked in accordance with author's experience and knowledge. Figure 13c, d depicts the comparative table, where machining is associated with the highest rank contributing to their lowest score for time and money. A study by Grzesiak et al. [144] compares traditional machining and hybrid processes involving additive manufacturing (AM) followed by machining. The findings suggest that for unit production, using hybrid processes with AM and machining is more cost-effective than traditional machining alone. These kinds of studies only prove significance of machining over other techniques in terms of functionality and cost.

Permanent prosthetics functioning as joint implant undergoes material wear because of being in continuous interaction. Metal on metal joints has the highest wear rate, whereas combinations of metal on poly, ceramics on poly, and ceramics with ceramics are currently in use which show higher wear resistance [145]. In healthy joints, synovial fluid

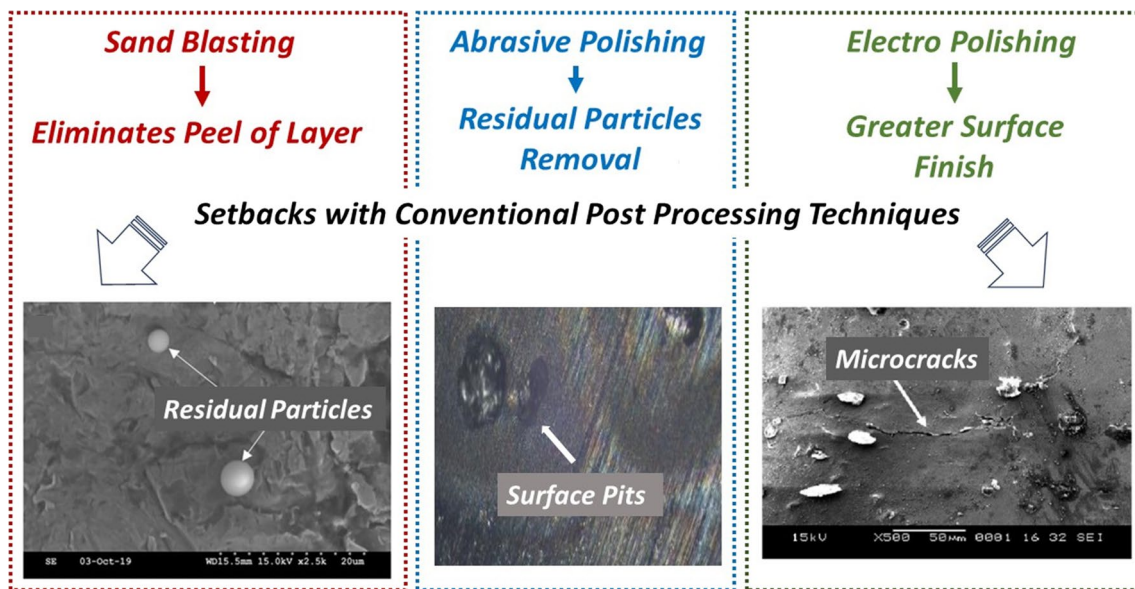


Fig. 12 Target objectives and setbacks of conventional post-processing techniques [142]

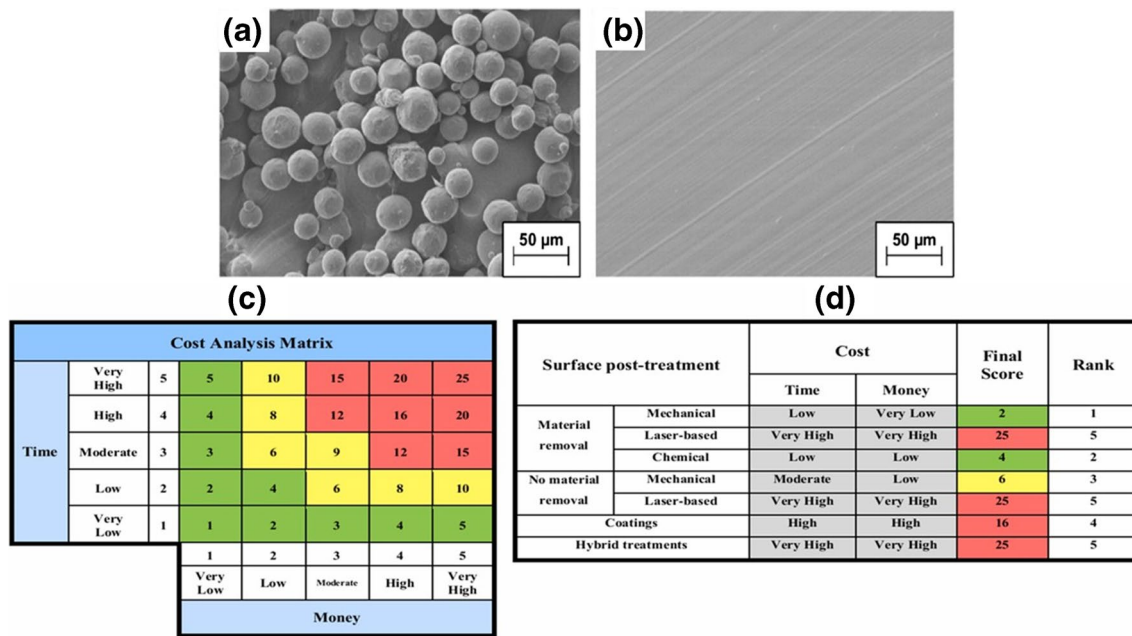


Fig. 13 a As-built 3D-printed surface with residual particles. b Machined part with no defects and high surface finish. c Cost analysis matrix for different post-processing techniques. d Mechanical machining ranked the highest for least time and money [143]

comprising an electrolyte solution of protein and lipid acts as a natural lubricant. Machining of micropits on the surface of joint implants has shown development of a mixed lubricating concept, these machined pits act as microhydrodynamic bearing [146]. Figure 14 shows microfeatures machined over metallic femoral head acting as a lubricating surface reducing direct contact and friction, resulting in reduced wear, and increased in-life span of hip implant[147].

Gokuldoss et al. [118] conducted a study on post-process machining of turning additively manufactured (AM) stainless steel, focusing on how machining parameters influence various properties crucial for medical applications. They examined the effects of cutting speed, depth of cut, and feed rate on porosity, surface quality, microstructure, and microhardness.

Figure 15 illustrates the impact of these machining parameters on the surface properties of AM parts. The machined parts showed an 88% reduction in surface roughness compared to as-printed stainless steel, as shown in Fig. 15a. Additionally, machining significantly affects microstructure and microhardness. The strain-hardened layer formed during machining reduces surface and subsurface porosity, enhancing the material's fatigue and wear resistance. Moreover, machining produces smaller grains on the surface, increasing microhardness, as depicted in Fig. 15b. With cutting speed, the size of cellular grains is also increasing as depicted in Fig. 15c. This refinement in microstructure is due to the increase in dislocation density, which is caused by the higher surface stress associated with increased cutting speed.

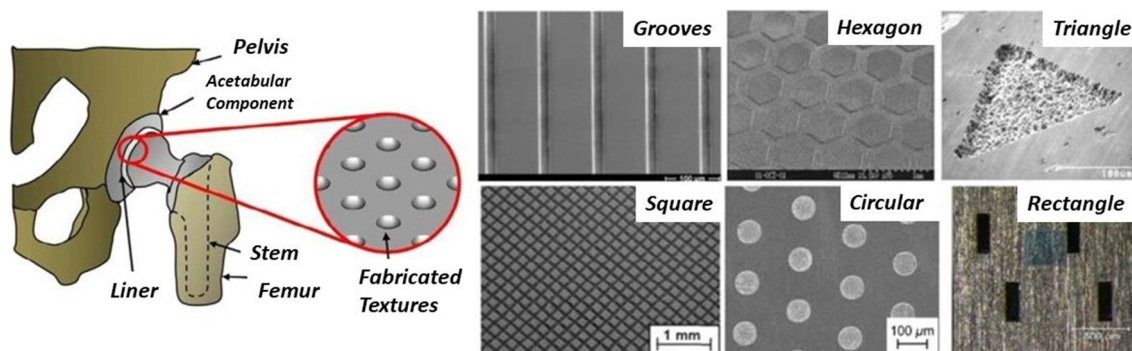
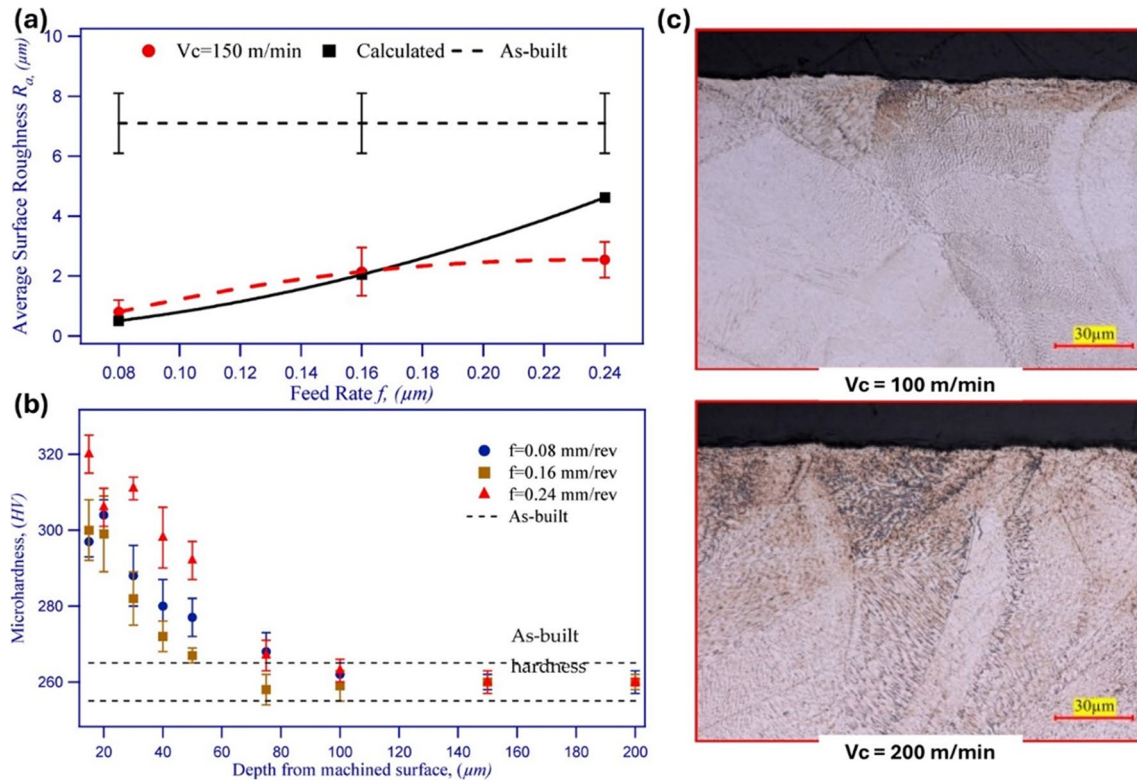


Fig. 14 Machined microfeatures reducing friction between metal-on-metal implants [148]



**Fig. 15** Effects of machining: **a** feed rate on surface roughness, **b** depth of cut on microhardness, and **c** cutting speed on microstructure—comparison of machined and as print stainless steel [140]

Therefore, machining not only improves surface roughness but also refines surface-level properties such as porosity, wear resistance, corrosion resistance, and microhardness. This highlights the capability of machining to enhance the overall performance of additively manufactured stainless steel for medical applications.

## 7 Effects of MAM parameters on functionality of orthopaedic implants

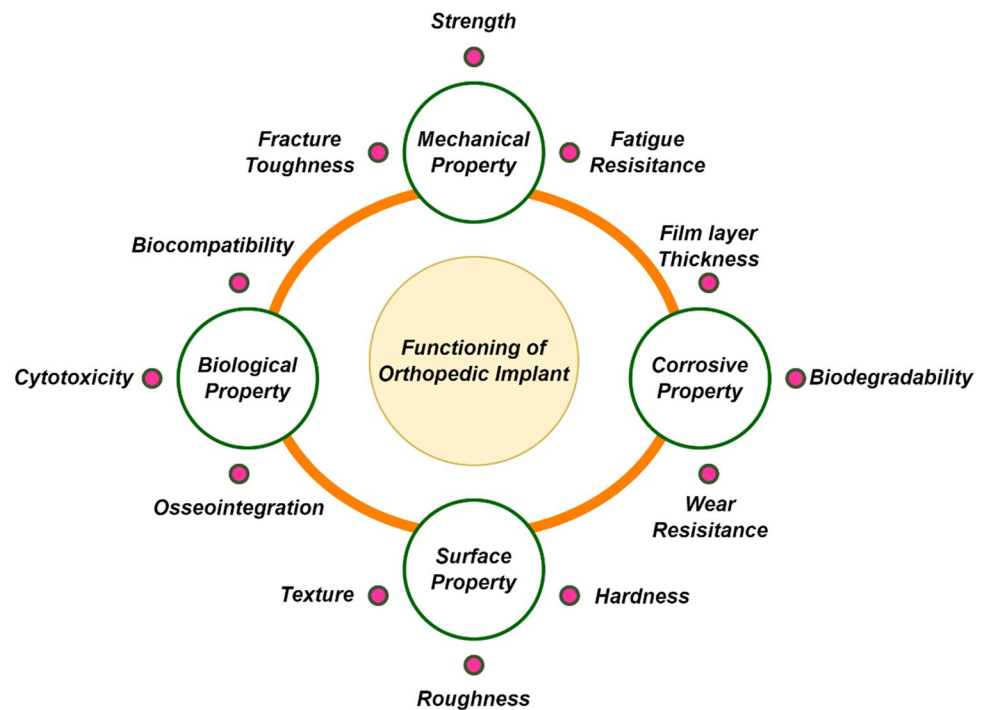
Biocompatibility of a material accounts for its ability to possess required biological, and functional properties to perform proficiently under demanding physiological conditions, without causing any detrimental response in the body [149]. Permanent implants require parts with wear and corrosive resistance, possessing mechanical properties matching cortical bone eliminating stress shielding. Bone grafting scaffolds are required to have mechanical properties matching cancellous or cortical bone depending on its area of usage. Temporary implants demand mechanical properties matching cortical bone with an ability to absorb/degrade in accordance to bone healing period. Apart from possessing mechanical and corrosive properties, these implants also require relevant biological properties to eliminate toxicity

and promote osseointegration [150]. Figure 16 represents essential properties required for effective functioning of an orthopaedic implant.

Biocompatibility of implants is function of material characteristics and their manufacturing process. MAM is a layer-by-layer processing techniques which induces anisotropic properties, where finish machining has considerable effect on surface property, corrosion, and fatigue. MAM process undergoes complex cyclic thermal history from directional heating, repetitive melting, fusion, and rapid solidification [151]. This induces directional changes in microstructure resulting in material heterogeneity and anisotropy. Process specific defects like pores, high surface roughness, and unfused layers also contribute to change in material properties [152].

MAM process parameters like deposition rate, beam size and power, build environment, processing temperature, and scanning strategy have effects on microstructure and functional property of additively manufactured material [157]. Figure 17a–d presents an overview on effects of different MAM process parameters on material anisotropy. Deposition or powder feed rate influences the nature of grain morphology. Wang et al. [153] noticed more equiaxed grain on laser melt deposition of titanium alloys with high deposition rate as depicted in Fig. 17a, where columnar grain increased

**Fig. 16** Vital properties for a functional orthopaedic implant [150]



with decrease of deposition rate. Larger melt pool geometry and higher scanning velocity resulted in development of higher equiaxed grain depicting this a process-dependent effect.

Unoptimised beam size and power can result in overheating or evaporation of metal powders. Keyhole porosity is welding like defect developed in MAM, due to vaporised bubble trapped in a metal pool [154]. Difference in process and gas induced porosity can be appreciated with Fig. 17b. Directional formation of such defects inherently affects materials, developing anisotropic property. Uncontrolled build environment in MAM can lead to absorption of impurities; this gives rise in need to regulate the process under inert gas or vacuum atmosphere. But increased pressure under very high vacuum environment can lead to increased vaporisation resulting in heterogeneity of material. Ferrar et al. [158] also presented effects of inert gas flow rate and pathway on porosity of MAM-processed material. Their study proved more consistent gas flow resulting in lesser porosity and better compressive property, for porous Ti manufactured through SLM.

Change and difference in processing and substrate temperature can give rise to high magnitude of residual stress. Wang et al. [159] characterised residual stress as an effect of processing temperatures and presented a heterogeneity along X and Y plane of EBM processed Ti-6Al-4 V. Variation in residual stress along different points in X and Y plane can be seen in Fig. 17c. Different modes of scanning strategies ranging from bi-directional, zig zag, and checker box are used in MAM. These scanning strategies influence crystal structure

as it effects direction of thermal gradient. Helmer et al. [156] presented dependence on formation of equiaxed or columnar grain on scanning strategy. Figure 17d is a microstructural image showing columnar and equiaxed grain morphologies resulting with difference in scanning strategy.

## 7.1 Managing defects in MAM—process control and heat treatment

Process-induced defects result in causing detrimental effects on fatigue life of MAM parts. With layer-by-layer manufacturing, process parameters play very crucial role on the microstructure and inherent related functional properties. Residual stress and anisotropy are such defects which are consequential part of rapid heat-cooling cycle in 3D-printed metallic part [160]. Scanning strategy and resultant differential cooling play a defining role for material anisotropy. Figure 18a represents a consequence of build-up residual stress, where a part distortion can occur during or post-build. EBM with slower cooling rates and pre-heated build plate result in development of parts with relatively reduced anisotropy and residual stress compared to SLM. Scanning strategies can effectively reduce residual stresses in Laser Additive Manufacturing (LAM). Zhan et al. [161] analysed effects of different scanning strategies as depicted in Fig. 18b, c, where island scanning showed 45% overall reduced residual stresses than line scanning strategy. Their study showed reduction in transverse residual stresses for LAM build Ti-6Al-4 V from 63.3 to 31.3 MPa, where longitudinal stress relaxation was from 281.4 to 124.6 MPa.

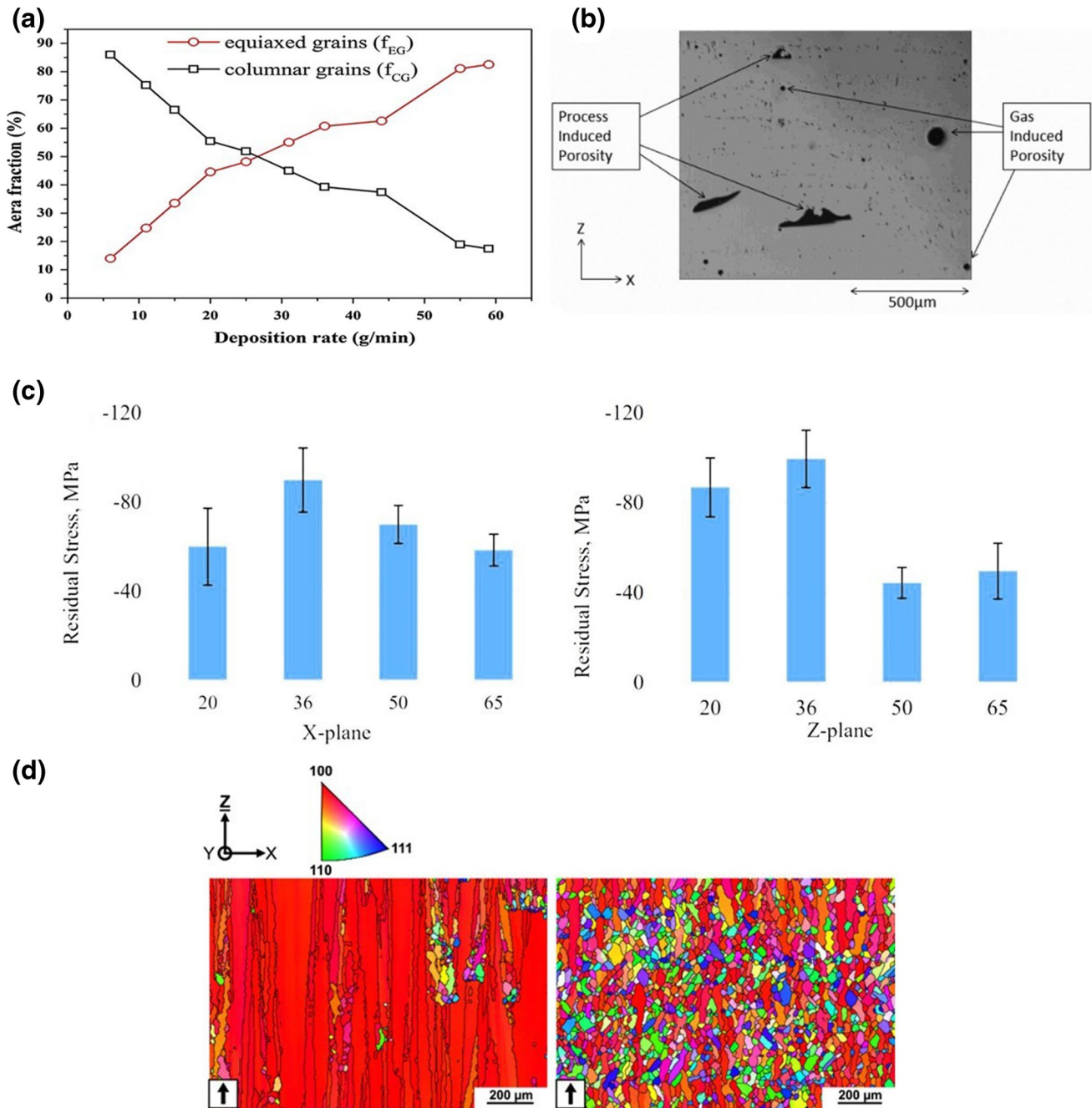


**Fig. 17** Effects of MAM process parameters on material properties: **a** deposition rate vs grain growth, **b** process-induced porosity, **c** non-homogeneous residual stress, and **d** effect of scan strategy on grain morphology [153–156]

Where process control can be beneficial for managing residual stress, heat treatment with high temperature and hold time can relax stresses resulting in more isotropic properties in the 3D-printed metals. Apart from relaxing stresses, post-process heat treatment is beneficial in modifying grain morphology, inducing precipitates, and recrystallization improving multiple functional properties [162]. Figure 19

signifies changes in (a) grain morphology, (b) precipitation and (c) residual stress with heat treatments of SLM-processed stainless steel, where grain size increased from 17.6 µm in as SLM part to 23 µm after heat treatment. Increased precipitations were noted along grain boundaries after heat treatment. Residual stresses also decreased along both transverse and longitudinal directions with heat treatment.

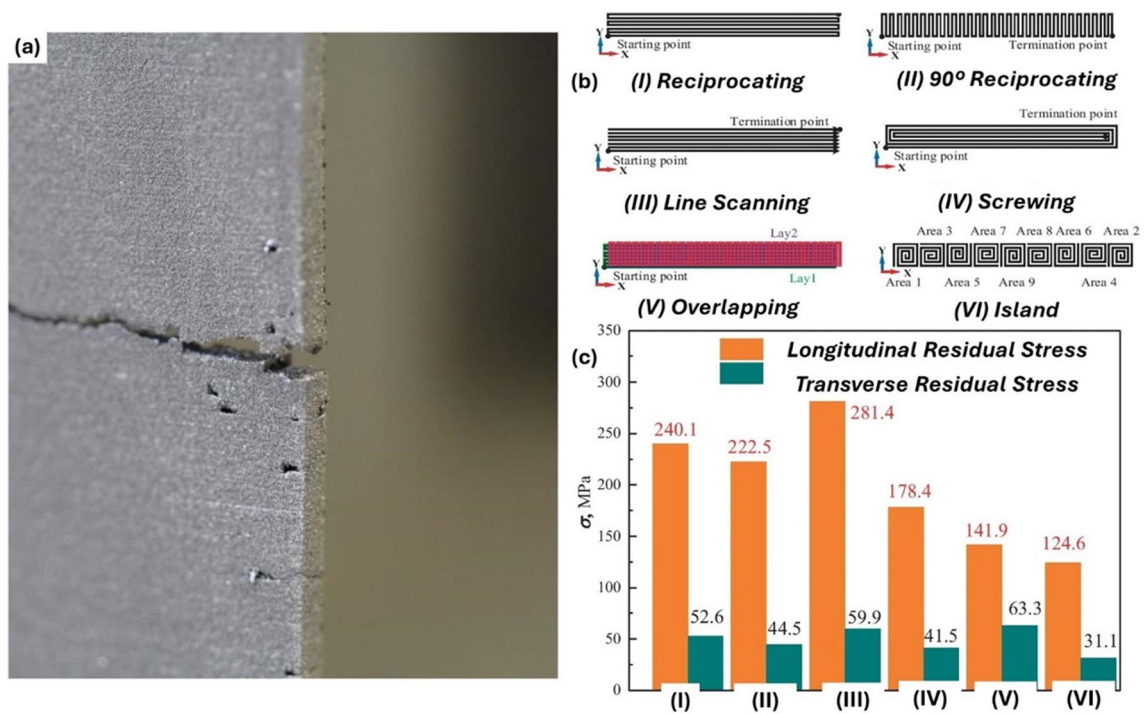


Fig. 18 a Build-up residual stress in SLM, b scanning strategies, and c effects of scanning strategies on residual stress [160, 161]

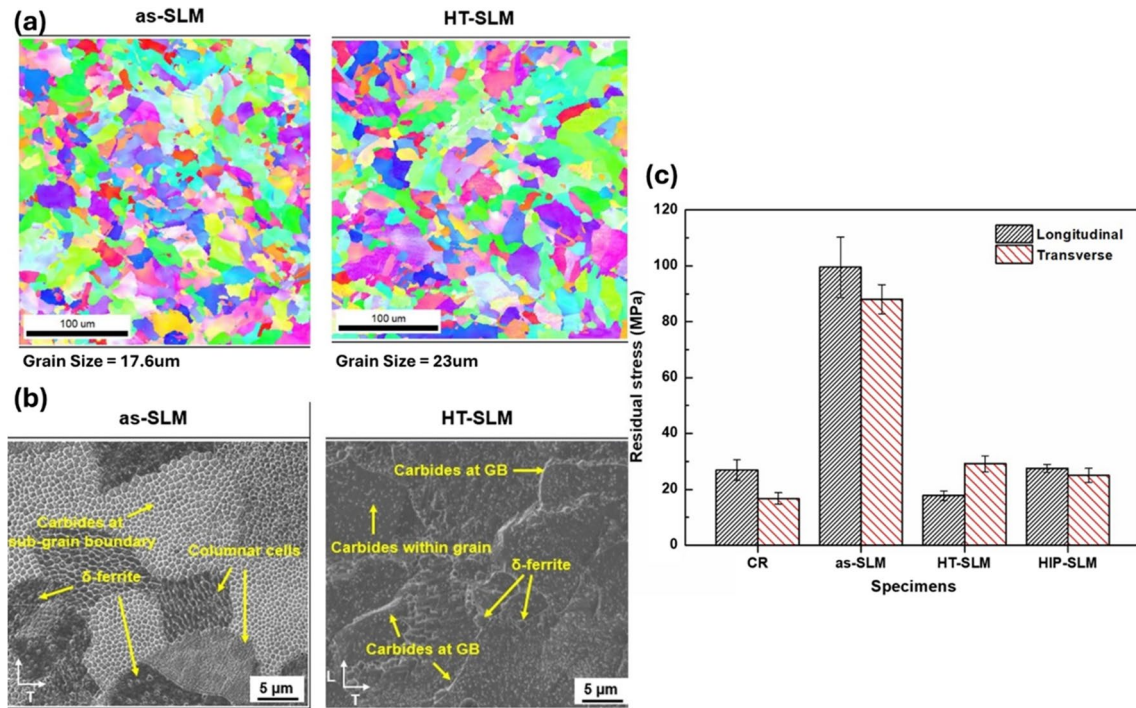


Fig. 19 Heat treatment effects on SLM: a grain size, b precipitation, and c residual stress [162]

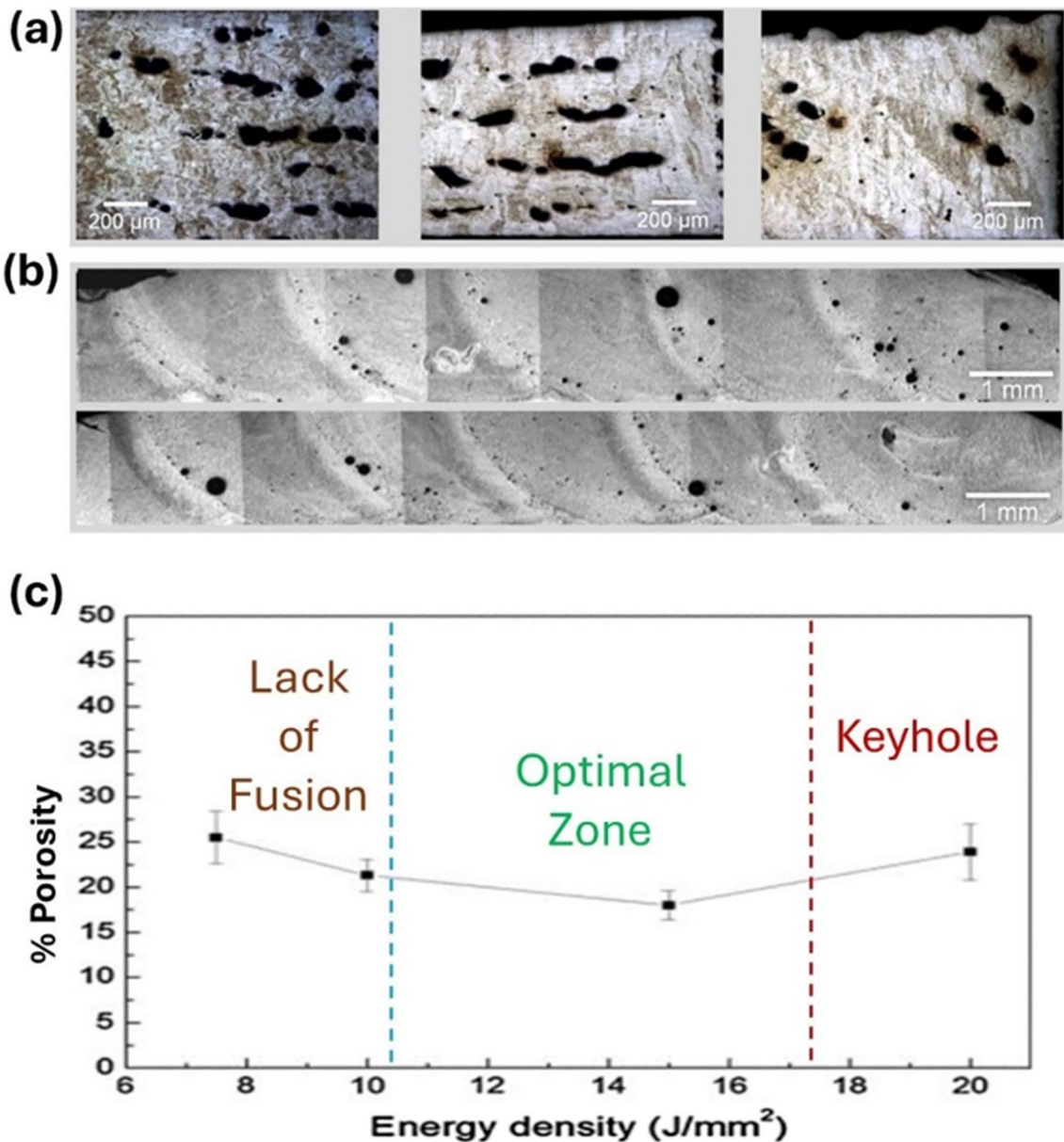


Fig. 20 Process defects: **a** lack of fusion, **b** gas pores, and **c** mitigation of defects with process control [163]

$$VED = \frac{P}{t \cdot d \cdot v} \quad (3)$$

As depicted in Fig. 20, microstructural defects like (a) lack of fusion and (b) gas pores can act as stress concentration points causing crack propagation. These kinds of defects can be mitigated by an effective process control. These defects are mainly a function of volume energy density in PBF and DED techniques. High energy laser and electron beam when not controlled efficiently can either vaporise the melt pool or cause un-melted gaps [163]. Volume energy density (VED), as signified in Eq. 3, is a function of beam power ( $P$ ), layer thickness ( $t$ ), hatching distance ( $d$ ), and scanning speed ( $v$ ),

where reducing  $P$  and likewise increase of  $t$ ,  $d$ , and  $v$  result in lack of fusion defects and increased  $P$  with reduced  $t$ ,  $d$ , and  $v$  caused gas pores. Figure 20c depicts a process control methodology, where an optimised window of volume energy density results in achieving best results with least process-induced microstructural defects.

## 7.2 Mechanical properties of MAM-processed orthopaedic implants

Depending on the location of application, orthopaedic implants of different types are subjected to environment susceptible to discrete loading conditions. For instance,

hip implants must handle high cyclic loads and provide both strength and flexibility, often using a titanium. Knee implants experience complex loads and require stability and wear resistance, typically featuring cobalt-chromium alloy components. Spinal implants must support axial loads and promote vertebral fusion, using materials like titanium cages. Each implant type is tailored to its unique mechanical demands to ensure optimal performance and longevity.

For clinical purposes, materials are tested with computational modelling, mechanical testing, and in vivo testing, comprising motion analysis and imaging. Implant strength, rigidity, endurance limit and fatigue resistance are imperative properties needed to be analysed for implementing them in biological system [164]. Individual or combination of tensile, compressive, bending, and shear test analysis characterises material for their capability as being used for specific orthopaedic application. Measurement of material fracture and deformation gives information about failure mode and limit for maximum stress before fracture, which is critical factor determining structural prominence of implants [165].

Overall, for an orthopaedic implant, stress shielding is a major factor limiting its application for permanent and temporary implant application. Mismatch of Young's modulus results in bone deterioration and implant loosening; progress of MAM has resulted in development of implants which possess Young's modulus matching cortical bone. Topologically optimised porous architecture and relative development of parts with less density have resulted in more suitable mechanical properties for implants.

Ti6Al4V, which has Young's modulus of 119 GPa, shows lesser values in order of  $93 \pm 2$  GPa when processed through additive manufacturing [168]. Moreover, functionally graded additively manufactured Ti6Al4V results in samples with Young's modulus of 2 to 9 GPa with yield strength of 53 to 392 MPa making it suitable for load-bearing applications [169]. Similar trends are noticed for other permanent implant materials like stainless steel, and cobalt chromium

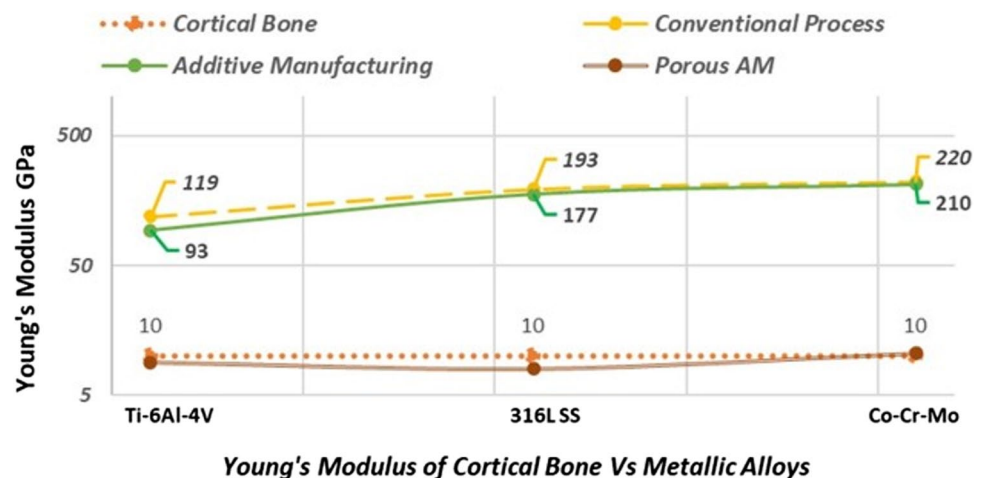
alloys [170, 171]. Figure 21 represents comparative analysis of Young's modulus for different materials when processed through route of conventional and additive manufacturing technology.

As noticed in Fig. 21, effect of changing scanning strategy and inducing anisotropy targeting reduction in stiffness is trivial to match cortical bone properties. Rather improvement in stiffness of metallic alloys making it comparable to cortical bone is achieved through spatial variation of porosity and pore sizes through additive manufacturing. MAM's capability to manufacture designs with different pore size enables in controlling mechanical properties of different materials [172, 173]. The study of Onal et al. [169] on mechanical property of functionally graded Ti-6Al-4 V shows that parts with smaller pores dimension of order 900  $\mu\text{m}$  in their cores and larger pore dimensions of 1000  $\mu\text{m}$  on outer shell jointly improve mechanical property and cell proliferation. Optimal mechanical properties are achieved by reduced stress concentration as function of varying pore dimensions, whereas outer shell with larger pore diameter attracts cell growth improving biocompatibility.

### 7.3 Corrosion properties of MAM-processed orthopaedic implants

Corrosion impacts functioning of orthopaedic devices by effecting structural integrity of permanent implants and biodegradability of temporary implants. Permanent prosthesis requires material with very low corrosion-induced wear, and temporary implant requires materials having suitable rate of corrosion for biodegradation to eliminate revision surgery [174]. Although additive manufacturing provides more suitable mechanical properties, rough surface produced by the process is susceptible to pitting corrosion. This makes post-processing necessary, especially for permanent implants. Mah et al. [175] characterised corrosive property of wrought and EBM manufactured Ti-6Al-4 V; their study

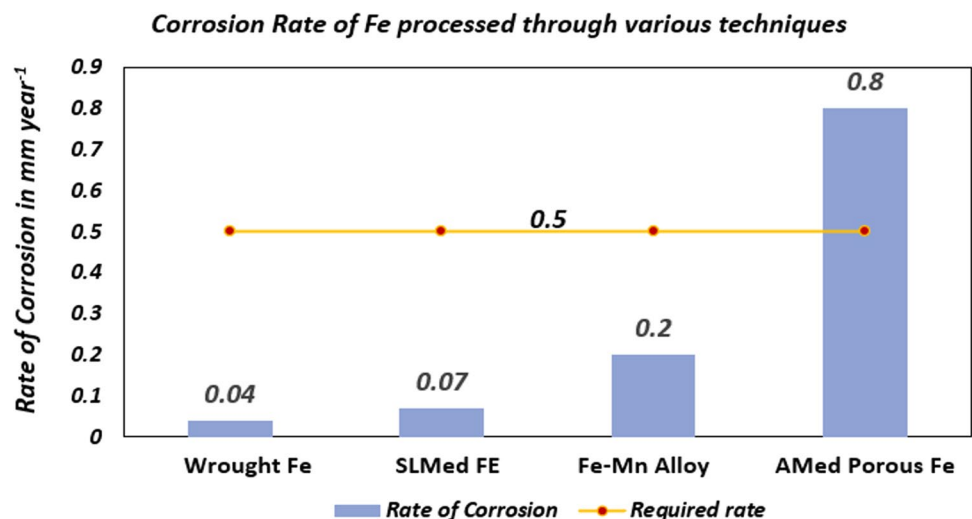
**Fig. 21** Comparison of Young's modulus of different material when processed through conventional and additive manufacturing technology [166, 167]



showed higher rate of corrosion in EBM manufactured material. Higher surface roughness measured on additively manufactured titanium leads to increase in corrosion. Although the rate of corrosion is under safety limit, but still due to higher susceptibility to pitting, these materials can have deteriorated mechanical property in long life. Parts produced with additive manufacturing possessing mechanical property matching cortical bone following surface modification or post-process machining having low surface roughness can be implemented for successful implementation of permanent implants [176].

Additive manufacturing has potential for developing biodegradable temporary implants. Mg, Fe, and Zn alloy systems have corrosion rate closer to the requirement presented by Erinc et al. [177]. Biodegradable fracture fixtures require corrosion resistance of  $0.5 \text{ mm year}^{-1}$  for effectively supporting fractured bone for their healing period of 4–6 months [177]. Although Zn presents closer degradation rate, their toxicity in the long run and difficulty in processing limit their application in additive manufacturing. Whereas, Mg can be processed with SLM, but it presents very high corrosion rate making it suitable only for non-load-bearing temporary implants. Fe based alloys have very low corrosion rate of  $0.04 \text{ mm year}^{-1}$ , which is not practical for biodegradable applications. Various research has been conducted to increase their corrosion rate by alloying with different elements, but the highest achievable rate was  $0.2 \text{ mm year}^{-1}$  [178]. Recently, with additive manufacturing functionally graded porous Fe materials were fabricated, which presented substantial mechanical property with corrosion rate of order  $0.8 \text{ mm year}^{-1}$  [128], making it practical for temporary implant application. Figure 22 represents corrosion rate of Fe alloys processed through conventional and additive manufacturing techniques.

**Fig. 22** Comparison of Fe corrosion rate processed through different techniques [128, 177, 178]



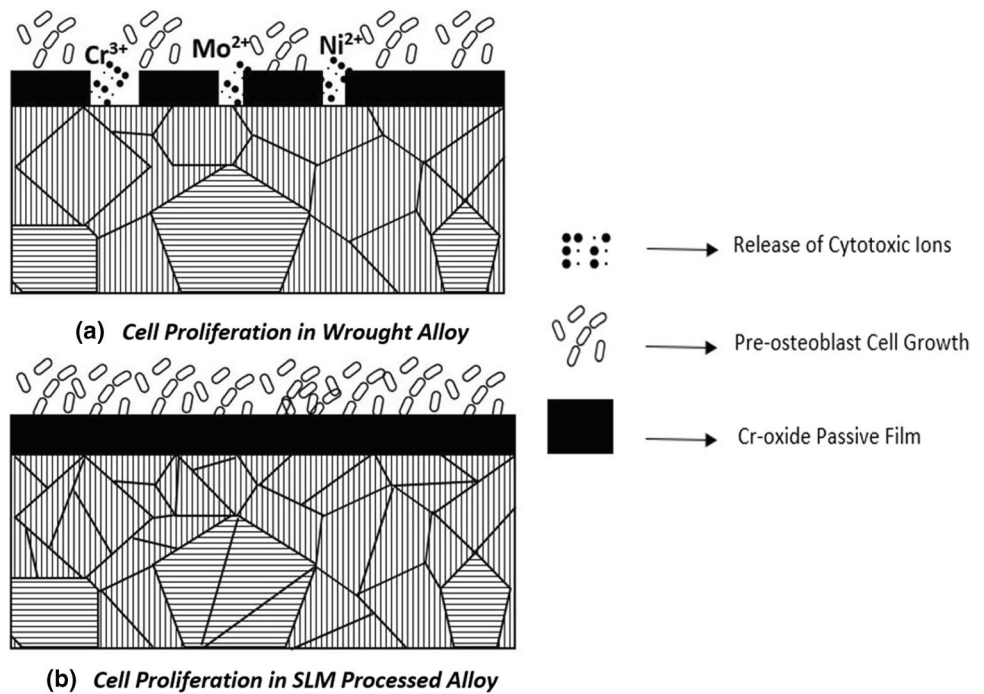
## 7.4 Biological properties of MAM-processed orthopaedic implants

Cell proliferation and adhesion are cell growth parameters which are affected by the surface quality of additive manufactured part. Roughness plays a vital role in adhesion of new cells over implant surface, whilst microstructure refinement influences cell proliferation. Elemental composition is another major factor affecting cytotoxicity and cell proliferation [179]. Mamun et al. [180] conducted a biocompatibility study on wrought and SLM-fabricated stainless steel, to compare their proliferation. Both alloys were treated to have similar surface topology. Their study revealed increased cell proliferation on additive manufactured stainless steel.

SLM-fabricated stainless steel showed higher density of MC3T3-E1 pre-osteoblast cells in order  $204 \pm 3 \text{ cells/mm}^2$ , compared to  $169 \pm 2 \text{ cells/mm}^2$  in wrought alloys [180]. Since both materials were treated to have similar surface topology and possessed the same chemical composition, difference in rate of cell growth is attributed to release of metal ions [181]. Stainless steel forms a thin passive layer of Cr-oxide under pathological conditions, which limit release of cytotoxic ions, promoting pre-osteoblast cell growth [182]. Rapid cooling rate in SLM-fabricated surface has more refined microstructure with sub grains stabilising passive film growth, thus improving biocompatibility of additive manufactured 316L SS. Figure 23a, b represents effects of microstructure on cell proliferation.

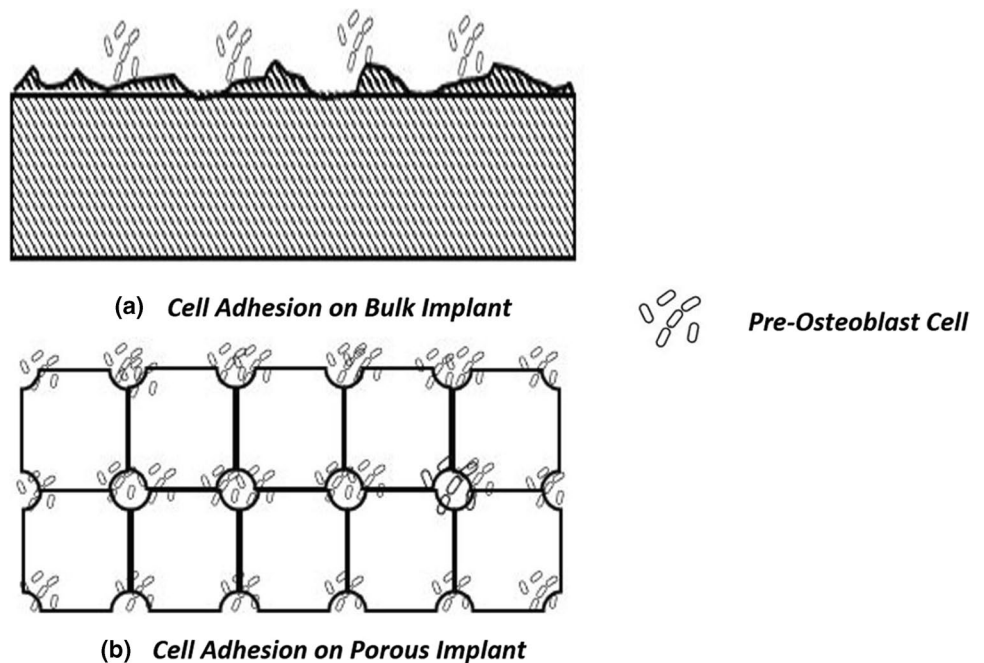
Surface conditioning is unavoidable step to improve biocompatibility of 3D-printed materials. Roughness value below  $2 \mu\text{m}$  is required for adequate cell adhesion on maxillofacial implant [183]. Although roughness plays a vital role in cell adhesion of bulk alloys, level of porosity and pore size are determining factors influencing cell growth in porous implants. Qin et al. [184] analysed cell adhesion and proliferation of MC3T3-E1 on bulk and porous biodegradable Zn-0.7Li. Growth of osteoblast cells was shrunk

**Fig. 23 a, b** Effects of micro-structure on cell proliferation of 316L SS [180]



in valleys and separated with peaks on bulk surface, where porous surface had laid out cells with interconnections. Qin et al. [184] characterised effects of pore size on cell adhesion of additive manufactured titanium implants. Their study analyses implants with pore size ranging from 300 to 900  $\mu\text{m}$ , porous design with 600  $\mu\text{m}$  resulted in promoting better cell ingrowth for permanent implant application. Figure 24a, b signifies difference in cell growth on bulk and porous surface.

**Fig. 24 a, b** Effects of surface on cell adhesion of biodegradable Zn-0.7Li [184]



## 8 Future directions

A clear understanding to proceed with defined preference will facilitate in guiding researchers to have specific direction on manufacturing implants whilst giving them more time to study and improve implant performance and functionality. Preference map with collated studies from this review aims to direct future research work focusing on development of

advanced orthopaedic implants. Figure 25 signifies impact of product design strategy with additive manufacturing over conservative process management approach.

MAM up to some extent overcomes the limitations in developing orthopaedic implants for permanent and temporary applications. Additively manufactured implants with engineered porous structure have shown great improvement in terms of possessing porosity with effective structural properties. However, MAM implants suffer from rough surfaces and are prone to corrosion, resulting in deterioration of mechanical properties in permanent applications. Also, there is a need to develop a clear methodology to analyse and study porous surfaces, as MAM parts are prone to porosity through both process and design. With regard to fracture fixation implants, a corrosion rate of 0.8 mm year<sup>-1</sup> has been achieved with development of porous Fe, but with an expense of reduced mechanical property. There is a need to develop a material which corrodes by maintaining sufficient mechanical property along bone healing period for 4–6 months. Mg and

Zn are other potential alloys which can be additively manufactured and analysed for temporary implant application.

With development of EBM and SLM, MAM presents competency in producing parts with wide range of materials with varied design strategies. Further prospects of MAM for orthopaedic implants can be analysed by a proposed two-way approach. Figure 26 represents a potential map which is developed with reference to different advanced manufacturing routes being employed with additive manufacturing by previous researchers [185–190]. Table 6 shows importance of the proposed approach.

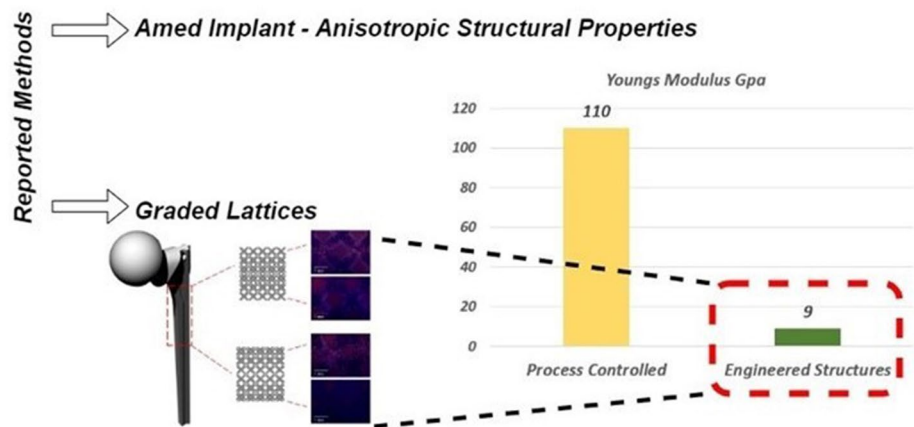
### 9 Conclusions

The primary goal of this review was to compile available material, manufacturing, and design techniques for the development of 3D-printed metallic orthopaedic implants,

Fig. 25 Preference map focusing studies on stress shielding and biodegradability, composed from [169] and [128]

#### Permanent Prosthesis

Determining Factor: Stress Shielding



#### Temporary Implants

Determining Factor: Biodegradability Eliminating Revision Surgery

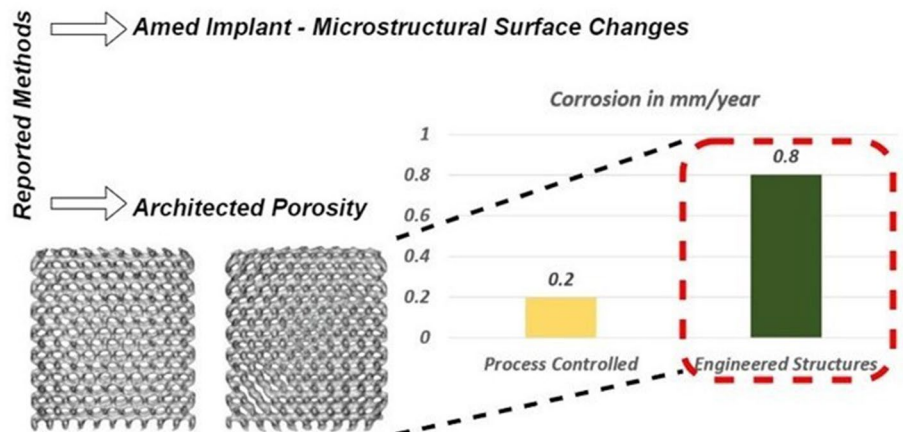


**Fig. 26** Prospects on additive manufacturing of orthopaedic implants, figure compiled with data from [185–190]

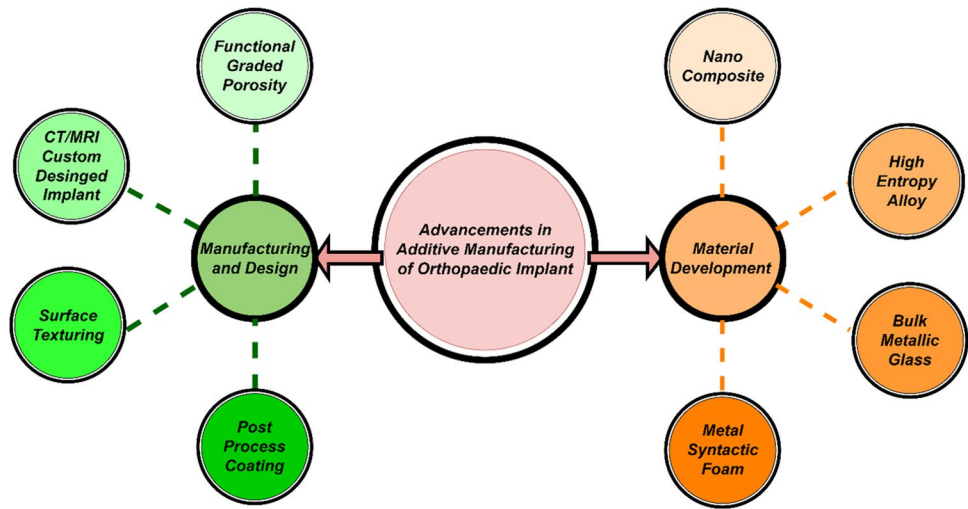


**Table 6** Significance of proposed approach

Material development approach		
Type of material	Significance	Reference
Nanocomposite	<ul style="list-style-type: none"> <li>• Addition of Ag and Au nano fibres improves antimicrobial properties</li> <li>• Graphene oxide fibres show increase in modulus and strength for porous materials</li> </ul>	[191, 192]
High entropy alloy	<ul style="list-style-type: none"> <li>• Additive manufactured HEA possess random crystal orientation providing unique material property</li> </ul>	[193, 194]
Bulk metallic glass	<ul style="list-style-type: none"> <li>• Additive manufactured BMG can be manufactured with no size constrains</li> <li>• Amorphous metals present control on corrosion and biodegradability</li> </ul>	[195]
Metal syntactic foam	<ul style="list-style-type: none"> <li>• Shows increased load-bearing capacity with porous material structure</li> </ul>	[196]
Manufacturing and design approach		
Development technique	Significance	Reference
Functional graded porosity	<ul style="list-style-type: none"> <li>• Presents biomimicry of bone with anisotropic structures</li> </ul>	[197]
CT/MRI direct 3D printing	<ul style="list-style-type: none"> <li>• Eliminates requirement of pre-operative bending/forming, facilitating use of brittle materials for implant</li> </ul>	[198, 199]
Coating	<ul style="list-style-type: none"> <li>• Promotes increased surface quality and cell proliferation</li> </ul>	[200]
Surface texturing	<ul style="list-style-type: none"> <li>• Post-process surface texturing presents reduction in friction for metal-on-metal prosthetics</li> </ul>	[201]

whilst briefly highlighting the significance of machining as a potentially best post-processing technique. Different MAM materials were reviewed, with titanium and stainless steel standing out as commercially ready materials with extensive research, making them simple to manufacture. Although there are other alloys with better functional properties, their commercial readiness is limited. Therefore, researchers should focus more on non-conventional alloy systems.

The ability of modified engineered designs to manage multiple properties, which can be used to tailor materials for specific requirements, shows great promise. With MAM, materials matching Young’s modulus close to 10 GPa are possible with controlled effect on stress shielding, where control on corrosion resistance ranging from 0.2 to 0.8 mm year<sup>-1</sup> is now possible making metallic implant suitable for biodegradable applications. However, whilst working with lattice structures, design for manufacturability is

critical. MAM can develop any complex design, but limited achievable tolerances and process uncertainty must be considered.

MAM has progressed significantly beyond its initial stage, with various power sources, processing methodologies, and feedstock-based systems developed, each with its own advantages. SLM, EBM, DED, and BJAM techniques are now being widely evaluated to produce orthopaedic implants to achieve maximum functionality and commercial benefit. Additional post-processing is an unavoidable step when using MAM. Therefore, studies on process strategies leading to MAM independence will result in significant relief for implant manufacturers.

Amongst available post-processing techniques, machining has proven commercial advantage due to its ability to remove multiple surface defects in one go, whilst also producing 88% lower surface roughness to a print part.

Comparatively with other post-processing methods multiple techniques would be required to remove each surface defect whilst also attempting to achieve set dimensional accuracy, and less surface roughness. Cellular designs, engineered lattice, and amorphous materials are gaining popularity; studies on the machinability of these additively manufactured devices will improve our understanding of their functionality and commercial readiness.

In summary, metal additive manufacturing emerges as a highly promising field for orthopaedic device developers. With its advanced process control and capacity to produce complex designs, MAM demonstrates its ability to manipulate various functional properties, including mechanical, corrosion resistance, and biological compatibility. As the field continues to evolve, the future promises even more intriguing developments, urging researchers to delve deeper into the intricacies of this transformative technique.

**Author contribution** The manuscript was chiefly authored by Mustafiz Shaikh, with Islam Shyha initiating the conceptualization of ideas and providing continuous input throughout all stages until final submission. Mohammad Alkhrisat conducted a technical review of medical terminology, whilst Zhilun Lu contributed with his expertise in material science. Fadi Kahwash and Ashfaq Mohammad conducted thorough reviews of process and design terminology. All authors participated in reviewing and approving the final version of the manuscript.

**Funding** This work was supported by Edinburgh Napier University, as the first author is a PhD candidate under studentship provided by the University in UKRI rate.

## Declarations

**Competing interests** The authors declare no competing interests.

**Open Access** This article is licensed under a Creative Commons Attribution 4.0 International License, which permits use, sharing, adaptation, distribution and reproduction in any medium or format, as long as you give appropriate credit to the original author(s) and the source, provide a link to the Creative Commons licence, and indicate if changes were made. The images or other third party material in this article are included in the article's Creative Commons licence, unless indicated otherwise in a credit line to the material. If material is not included in the article's Creative Commons licence and your intended use is not permitted by statutory regulation or exceeds the permitted use, you will need to obtain permission directly from the copyright holder. To view a copy of this licence, visit <http://creativecommons.org/licenses/by/4.0/>.

## References

1. *Standard terminology for additive manufacturing technologies*. Astm International, 2012. [Online]. Available: <https://www.astm.org/f2792-12.html>
2. Dutta B, Babu S, Jared B (2019) Chapter 1 - metal additive manufacturing. In: Dutta B, Babu S, Jared B (eds) Additive manufacturing materials and technologies, science, technology and applications of metals in additive manufacturing. Elsevier, pp 1–10. <https://doi.org/10.1016/B978-0-12-816634-5.00001-7>
3. Herzog D, Seyda V, Wycisk E, Emmelmann C (2016) Additive manufacturing of metals. *Acta Mater* 117:371–392. <https://doi.org/10.1016/j.actamat.2016.07.019>
4. Chen C, Shen Y, Tsai HL (2017) “A foil-based additive manufacturing technology for metal parts.” *J Manuf Sci Eng Trans ASME* 139:2. <https://doi.org/10.1115/1.4034139>
5. Bai L, Gong C, Chen X, Sun Y, Zhang J, Cai L, Zhu S, Xie SQ (2019) Additive manufacturing of customized metallic orthopedic implants: materials, structures, and surface modifications. *Metals* 9:1004. <https://doi.org/10.3390/met9091004>
6. Wang J-L, Xu J, Hopkins C, Chow D, Kiu H, Qin L (2020) Biodegradable magnesium-based implants in orthopedics—a general review and perspectives. *Adv Sci*:7. <https://doi.org/10.1002/adv.201902443>
7. Grammatopoulos G, Munemoto M, Pollalis A, Athanasou NA (2017) Correlation of serum metal ion levels with pathological changes of ARMD in failed metal-on-metal-hip-resurfacing arthroplasties. *Arch Orthop Trauma Surg* 137(8):1129–1137. <https://doi.org/10.1007/s00402-017-2723-x>
8. Wang M “Springer series in biomaterials science and engineering volume 4 series editor.” [Online]. Available: <http://www.springer.com/series/10955>
9. Zaborski S, Sudzik A, Wołyniec A (2011) Electrochemical polishing of total hip prostheses. *Arch Civil Mech Eng* 11(4):1053–1062. [https://doi.org/10.1016/s1644-9665\(12\)60095-8](https://doi.org/10.1016/s1644-9665(12)60095-8)
10. Lopes T, Silva P, Leal N, Neto R, Reis A (2012) Designing and manufacturing of custom hip prostheses by integrating casting technology. *J Biomech* 45:S289. [https://doi.org/10.1016/S0021-9290\(12\)70290-7](https://doi.org/10.1016/S0021-9290(12)70290-7)
11. Arabnejad S, Johnston B, Tanzer M, Pasini D (2017) Fully porous 3D printed titanium femoral stem to reduce stress-shielding following total hip arthroplasty. *J Orthop Res* 35(8):1774–1783. <https://doi.org/10.1002/jor.23445>
12. Cronskär M, Bäckström M, Rännar LE (2013) Production of customized hip stem prostheses - a comparison between conventional machining and electron beam melting (EBM). *Rapid Prototyp J* 19(5):365–372. <https://doi.org/10.1108/RPJ-07-2011-0067>
13. Zhang L, Kiat E, Pramanik A (2009) A briefing on the manufacture of hip joint prostheses. *Adv Mater Res* 76–78:212–216. <https://doi.org/10.4028/www.scientific.net/AMR.76-78.212>
14. Markopoulos AP, Galanis NI, Karkalos NE, Manolakos DE (2018) Precision CNC machining of femoral component of knee implant: a case study. *Machines* 6:1. <https://doi.org/10.3390/MACHINES6010010>
15. Shao H et al (2021) “Manufacturing of biodegradable intramedullary nail with high strength”, in Volume 1: Additive Manufacturing; Advanced Materials Manufacturing; Biomanufacturing; Life Cycle Engineering; Manufacturing Equipment and Automation. *Am Soc Mech Eng*. <https://doi.org/10.1115/MSEC2021-63654>
16. Murr LE et al (2010) Next-generation biomedical implants using additive manufacturing of complex, cellular and functional mesh arrays. *Phil Trans Royal Soc A: Math, Phys Eng Sci* 368(1917):1999–2032. <https://doi.org/10.1098/rsta.2010.0010>
17. Mobarak MH et al (2023) Recent advances of additive manufacturing in implant fabrication – a review. *Appl Surf Sci Adv* 18:100462. <https://doi.org/10.1016/j.apsadv.2023.100462>
18. Javaid M, Haleem A (2018) Additive manufacturing applications in orthopaedics: a review. *J Clin Orthop Trauma* 9(3):202–206. <https://doi.org/10.1016/j.jcot.2018.04.008>
19. Wu Y et al (2023) An overview of 3D printed metal implants in orthopedic applications: present and future perspectives. *Heliyon* 9(7):e17718. <https://doi.org/10.1016/j.heliyon.2023.e17718>

20. Millis D (2004) Responses of musculoskeletal tissues to disuse and remobilization. In: Canine rehabilitation and physical therapy, 2nd edn, pp 113–159. <https://doi.org/10.1016/B978-0-7216-9555-6.50011-5>
21. Kohn DH (2011) Porous coatings in orthopedics porous coatings in orthopedics. *Comprehensive Biomaterials* 6:65–77. <https://doi.org/10.1016/B978-0-08-055294-1.00201-4>
22. Tong X et al (2024) Degradable Zn–5Ce alloys with high strength, suitable degradability, good cytocompatibility, and osteogenic differentiation fabricated via hot-rolling, hot-extrusion, and high-pressure torsion for potential load-bearing bone-implant application. *J Market Res* 28:1752–1763. <https://doi.org/10.1016/j.jmrt.2023.12.098>
23. Imwinkelried T (2015) Testing the mechanical properties of surface-modified magnesium and magnesium alloys for biomedical applications. In: Surface modification of magnesium and its alloys for biomedical applications, vol 1, Woodhead Publishing, Oxford, pp. 311–329. <https://doi.org/10.1016/B978-1-78242-077-4.00010-3>
24. Munyensanga P, Bricha M, El Mabrouk K (2024) Functional characterization of biomechanical loading and biocorrosion resistance properties of novel additively manufactured porous CoCrMo implant: comparative analysis with gyroid and rhombic dodecahedron. *Mater Chem Phys* 316:129139. <https://doi.org/10.1016/j.matchemphys.2024.129139>
25. Jin W, Chu PK (2019) Orthopedic implants. In: Narayan R (ed) *Encyclopedia of biomedical engineering*. Elsevier, pp 425–439. <https://doi.org/10.1016/B978-0-12-801238-3.10999-7>
26. Li HF, Zheng YF (2016) Recent advances in bulk metallic glasses for biomedical applications. *Acta Biomaterialia* 36:1–20. <https://doi.org/10.1016/j.actbio.2016.03.047>
27. Farrow L, McLoughlin J, Gaba S, Ashcroft GP (2023) Future demand for primary hip and knee arthroplasty in Scotland. *Musculoskelet Care* 21(2):355–361. <https://doi.org/10.1002/msc.1701>
28. Arbab D, König DP (2016) Atraumatic femoral head necrosis in adults. *Dtsch Arztebl Int*. <https://doi.org/10.3238/arztebl.2016.0031>
29. Kurtz S, Lau E, Ong K, Zhao K, Kelly M, Bozic K (2009) Future young patient demand for primary and revision joint replacement: national projections from 2010 to 2030. *Clin Orthop Relat Res* 467:2606–2612. <https://doi.org/10.1007/s11999-009-0834-6>
30. Marsell R, Einhorn TA (2011) The biology of fracture healing. *Injury* 42(6):551–555. <https://doi.org/10.1016/j.injury.2011.03.031>
31. Smit T, Engels T, Söntjens S, Govaert L (2009) Time-dependent failure in load-bearing polymers: a potential hazard in structural applications of polylactides. *Journal of materials science. J Mater Sci: Mater Med* 21:871–878. <https://doi.org/10.1007/s10856-009-3921-z>
32. Antoniac I et al (2022) “Magnesium-based alloys used in orthopedic surgery,” MDPI. <https://doi.org/10.3390/ma15031148>
33. Margerrison E, Argentieri M, Schoelles K, Lucas SR “magnesium safety profile report details date of submission ECRI Corporate Governance Project Manager,” 2021. [Online]. Available: <https://www.fda.gov/media/152349/download>
34. US Food and Drug Administration, “Biological responses to metal implants,” 2019. [Online]. Available: <https://www.fda.gov/media/131150/download>
35. Li B, Webster T (2018) Orthopedic biomaterials progress in biology, manufacturing, and industry perspectives. *Springer Int Publ*. <https://doi.org/10.1007/978-3-319-89542-0>
36. Manivasagam G, Singh AK, Rajamanickam A, Gogia A (2009) Ti based biomaterials, the ultimate choice for orthopaedic implants – a review. *Prog Mater Sci* 54:397–425. <https://doi.org/10.1016/j.pmatsci.2008.06.004>
37. Gaytan SM et al (2010) Comparison of microstructures and mechanical properties for solid and mesh cobalt-base alloy prototypes fabricated by electron beam melting. *Metall Mater Trans A Phys Metall Mater Sci* 41(12):3216–3227. <https://doi.org/10.1007/s11661-010-0388-y>
38. Milošev I, Levašič V, Kovač S, Sillat T, Virtanen S, Tiainen V-M, Trebše R (2021) Metals for joint replacement. In: Revell P (ed) *Joint replacement technology*, 3rd edn. Woodhead Publishing, pp 65–122. <https://doi.org/10.1016/B978-0-12-821082-6.00020-0>
39. Zhong Y, Liu L, Wikman S, Cui D, Shen Z (2016) Intragranular cellular segregation network structure strengthening 316L stainless steel prepared by selective laser melting. *J Nucl Mater* 470:170–178. <https://doi.org/10.1016/j.jnucmat.2015.12.034>
40. Murr LE, Quinones SA, Gaytan SM, Lopez MI, Rodela A, Martinez EY, Hernandez DH, Martinez E, Medina F, Wicker RB (2009) Microstructure and mechanical behavior of Ti–6Al–4V produced by rapid-layer manufacturing, for biomedical applications. *J Mech Behav Biomed Mater* 2(1):20–32. <https://doi.org/10.1016/j.jmbbm.2008.05.004>
41. Zhong Y et al (2017) Additive manufacturing of 316L stainless steel by electron beam melting for nuclear fusion applications. *J Nucl Mater* 486:234–245. <https://doi.org/10.1016/j.jnucmat.2016.12.042>
42. Sherepo KM, Red'ko IA (2004) Use of zirconium-based and zirconium-coated implants in traumatology and orthopedics. *Biomed Eng (NY)* 38(2):77–79. <https://doi.org/10.1023/B:BIEN.0000035726.31175.f8>
43. Sahasrabudhe H, Bandyopadhyay A (2018) Laser-based additive manufacturing of zirconium. *Appl Sci (Switzerland)* 8:3. <https://doi.org/10.3390/app8030393>
44. Sahasrabudhe H, Bandyopadhyay A (2016) Additive manufacturing of reactive in situ Zr based ultra-high temperature ceramic composites. *JOM* 68(3):822–830. <https://doi.org/10.1007/s11837-015-1777-x>
45. Xie J, Huang Z, Lu H, Zheng B, Xu X, Lei J (2021) Additive manufacturing of tantalum-zirconium alloy coating for corrosion and wear application by laser directed energy deposition on Ti6Al4V. *Surf Coat Technol* 411:127006. <https://doi.org/10.1016/j.surfcoat.2021.127006>
46. Yang H et al (2020) Alloying design of biodegradable zinc as promising bone implants for load-bearing applications. *Nat Commun* 11:1. <https://doi.org/10.1038/s41467-019-14153-7>
47. Sekar P, Narendranath S, Desai V (2021) Recent progress in in vivo studies and clinical applications of magnesium based biodegradable implants – a review. *J Magnes Alloys* 9(4):1147–1163. <https://doi.org/10.1016/j.jma.2020.11.001>
48. Zamani Y et al (2021) A review of additive manufacturing of Mg-based alloys and composite implants. *J Compos Comp* 2(5):71–83. <https://doi.org/10.52547/jcc.3.1.7>
49. Esmaily M et al (2020) A detailed microstructural and corrosion analysis of magnesium alloy WE43 manufactured by selective laser melting. *Addit Manuf* 35:101321. <https://doi.org/10.1016/j.addma.2020.101321>
50. Wegener B et al (2020) Development of a novel biodegradable porous iron-based implant for bone replacement. *Sci Rep* 10:1. <https://doi.org/10.1038/s41598-020-66289-y>
51. Li Y et al (2019) Additively manufactured functionally graded biodegradable porous iron. *Acta Biomater* 96:646–661. <https://doi.org/10.1016/j.actbio.2019.07.013>
52. Chen Y et al (2016) Comparative corrosion behavior of Zn with Fe and Mg in the course of immersion degradation in phosphate buffered saline. *Corros Sci* 111:541–555. <https://doi.org/10.1016/j.corsci.2016.05.039>
53. Lietaert K et al (2020) Mechanical properties and cytocompatibility of dense and porous Zn produced by laser powder bed

- fusion for biodegradable implant applications. *Acta Biomater* 110:289–302. <https://doi.org/10.1016/j.actbio.2020.04.006>
54. Demir AG, Monguzzi L, Previtali B (2017) Selective laser melting of pure Zn with high density for biodegradable implant manufacturing. *Addit Manuf* 15:20–28. <https://doi.org/10.1016/j.addma.2017.03.004>
  55. Bartolomeu F et al (2017) 316L stainless steel mechanical and tribological behavior—a comparison between selective laser melting, hot pressing and conventional casting. *Addit Manuf* 16:81–89. <https://doi.org/10.1016/j.addma.2017.05.007>
  56. Gor M, Soni H, Singh Rajput G, Sahlot P (2022) Experimental investigation of mechanical properties for wrought and selective laser melting additively manufactured SS316L and MS300. *Mater Today Proc* 62:7215–7219. <https://doi.org/10.1016/j.matpr.2022.03.511>
  57. Lodhi MJK, Deen KM, Greenlee-Wacker MC, Haider W (2019) Additively manufactured 316L stainless steel with improved corrosion resistance and biological response for biomedical applications. *Addit Manuf* 27:8–19. <https://doi.org/10.1016/j.addma.2019.02.005>
  58. Fischer RD, Klasen J, Shmatok A, Prorok BC (2021) An additively manufactured locking fixation system for potential application in patient-specific implants. *J Mech Behav Biomed Mater* 124:104867. <https://doi.org/10.1016/j.jmbbm.2021.104867>
  59. Mohd Yusuf S, Lim D, Chen Y, Yang S, Gao N (2021) Tribological behaviour of 316L stainless steel additively manufactured by laser powder bed fusion and processed via high-pressure torsion. *J Mater Process Technol* 290:116985. <https://doi.org/10.1016/j.jmatprotec.2020.116985>
  60. Bhardwaj T, Shukla M, Paul CP, Bindra KS (2019) Direct energy deposition - laser additive manufacturing of titanium-molybdenum alloy: parametric studies, microstructure and mechanical properties. *J Alloys Compd* 787:1238–1248. <https://doi.org/10.1016/j.jallcom.2019.02.121>
  61. Wysocki B, Maj P, Sitek R, Buhagiar J, Kurzydłowski KJ, Świeszkowski W (2017) Laser and electron beam additive manufacturing methods of fabricating titanium bone implants. *Appl Sci (Switzerland)* 7:7. <https://doi.org/10.3390/app7070657>
  62. England T, Pagkalos J, Jeys L, Botchu R, Carey Smith R (2021) Additive manufacturing of porous titanium metaphyseal components: early osseointegration and implant stability in revision knee arthroplasty. *J Clin Orthop Trauma* 15:60–64. <https://doi.org/10.1016/j.jcot.2020.10.042>
  63. Regis M, Marin E, Fedrizzi L, Pressacco M (2015) Additive manufacturing of trabecular titanium orthopedic implants. *MRS Bull* 40(2):137–144. <https://doi.org/10.1557/mrs.2015.1>
  64. Eldesouky I, Harrysson O, West H, Elhofy H (2017) Electron beam melted scaffolds for orthopedic applications. *Addit Manuf* 17:169–175. <https://doi.org/10.1016/j.addma.2017.08.005>
  65. Ahn YK et al (2017) Mechanical and microstructural characteristics of commercial purity titanium implants fabricated by electron-beam additive manufacturing. *Mater Lett* 187:64–67. <https://doi.org/10.1016/j.matlet.2016.10.064>
  66. Ameen W, Al-Ahmari A, Mohammed MK, Abdulhameed O, Umer U, Moiduddin K (2018) Design, finite element analysis (FEA), and fabrication of custom titanium alloy cranial implant using electron beam melting additive manufacturing. *Advin Prod Eng Manage* 13(3):267–278. <https://doi.org/10.14743/apem2018.3.289>
  67. Han C et al (2017) Effects of the unit cell topology on the compression properties of porous Co-Cr scaffolds fabricated via selective laser melting. *Rapid Prototyp J* 23(1):16–27. <https://doi.org/10.1108/RPJ-08-2015-0114>
  68. Suresh G, Narayana KL, Kedar Mallik M (2018) “Bio-compatible processing of LENS TM Deposited Co-Cr-W alloy for medical applications,” [Online]. Available: [www.sciencepubco.com/index.php/IJET](http://www.sciencepubco.com/index.php/IJET)
  69. Xiang DD et al (2019) Anisotropic microstructure and mechanical properties of additively manufactured Co–Cr–Mo alloy using selective electron beam melting for orthopedic implants. *Mater Sci Eng A* 765:138270. <https://doi.org/10.1016/j.msea.2019.138270>
  70. Stenlund P et al (2015) Osseointegration enhancement by Zr doping of Co-Cr-Mo implants fabricated by electron beam melting. *Addit Manuf* 6:6–15. <https://doi.org/10.1016/j.addma.2015.02.002>
  71. Iatecola A et al (2021) Osseointegration improvement of co-crm alloy produced by additive manufacturing. *Pharmaceutics* 13:5. <https://doi.org/10.3390/pharmaceutics13050724>
  72. Mohsan AUH, Wei D (2023) Advancements in additive manufacturing of tantalum via the laser powder bed fusion (LPBF): a comprehensive review. *Materials* 16(19):6419. <https://doi.org/10.3390/ma16196419>
  73. Aliyu AAA et al (2023) Additive manufacturing of tantalum scaffolds: processing, microstructure and process-induced defects. *Int J Refract Metals Hard Mater* 112:106132. <https://doi.org/10.1016/j.ijrmhm.2023.106132>
  74. Sungail C, Abid AD (2020) Additive manufacturing of tantalum – a study of chemical and physical properties of printed tantalum. *Met Powder Rep* 75(1):28–33. <https://doi.org/10.1016/j.mprp.2019.03.001>
  75. Harooni A, Irvani M, Khajepour A, King JM, Khalifa A, Gerlich AP (2018) Mechanical properties and microstructures in zirconium deposited by injected powder laser additive manufacturing. *Addit Manuf* 22:537–547. <https://doi.org/10.1016/j.addma.2018.05.037>
  76. Torun G et al (2022) Microstructure and mechanical properties of MRI-compatible Zr-9Nb-3Sn alloy fabricated by a laser powder bed fusion process. *Addit Manuf* 52:102647. <https://doi.org/10.1016/j.addma.2022.102647>
  77. Yue M, Liu Y, He G, Lian L (2022) Microstructure and mechanical performance of zirconium, manufactured by selective laser melting. *Mater Sci Eng, A* 840:142900. <https://doi.org/10.1016/j.msea.2022.142900>
  78. Issariyapat A et al (2023) Microstructure refinement and strengthening mechanisms of additively manufactured Ti-Zr alloys prepared from pre-mixed feedstock. *Addit Manuf* 73:103649. <https://doi.org/10.1016/j.addma.2023.103649>
  79. Farag MM, Yun HS (2014) Effect of gelatin addition on fabrication of magnesium phosphate-based scaffolds prepared by additive manufacturing system. *Mater Lett* 132:111–115. <https://doi.org/10.1016/j.matlet.2014.06.055>
  80. Liu C, Zhang M, Chen C (2017) Effect of laser processing parameters on porosity, microstructure and mechanical properties of porous Mg-Ca alloys produced by laser additive manufacturing. *Mater Sci Eng, A* 703:359–371. <https://doi.org/10.1016/j.msea.2017.07.031>
  81. Allavikuty R, Gupta P, Santra T, Rengaswamy J (2021) Additive manufacturing of Mg alloys for biomedical applications: current status and challenges. *Curr Opin Biomed Eng* 18:100276. <https://doi.org/10.1016/j.cobme.2021.100276>
  82. Behera M, Panemangalore DB, Shabadi R (2021) Additively manufactured magnesium-based bio-implants and their challenges. *Trans Indian Nat Acad Eng* 6(4):917–932. <https://doi.org/10.1007/s41403-021-00241-y>
  83. Sezer N, Evis Z, Koç M (2021) Additive manufacturing of biodegradable magnesium implants and scaffolds: Review of the recent advances and research trends. *J Magnes Alloys* 9(2):392–415. <https://doi.org/10.1016/j.jma.2020.09.014>
  84. Shuai C, Cheng Y, Yang Y, Peng S, Yang W, Qi F (2019) Laser additive manufacturing of Zn-2Al part for bone repair:

- formability, microstructure and properties. *J Alloys Compd* 798:606–615. <https://doi.org/10.1016/j.jallcom.2019.05.278>
85. Chen Y et al (2019) Laser additive manufacturing of Zn metal parts for biodegradable implants: effect of gas flow on evaporation and formation quality. *J Laser Appl* 31(2):022304. <https://doi.org/10.2351/1.5096118>
  86. Qin Y et al (2019) Additive manufacturing of biodegradable Zn-xWE43 porous scaffolds: formation quality, microstructure and mechanical properties. *Mater Des* 181:107937. <https://doi.org/10.1016/j.matdes.2019.107937>
  87. Voshage M, Wen P, Schaukellis M, Schleifenbaum JH (2019) Formation quality, mechanical properties, and processing behavior of pure zinc parts produced by laser-based manufacturing for biodegradable implants. *BHM Berg- Huettenmaenn Monatsh* 164(3):133–140. <https://doi.org/10.1007/s00501-019-0829-x>
  88. Youwen Y, Guoqing C, Mingli Y, Dongsheng W, Shuping P, Zhigang L, Cijun S (2021) Laser additively manufactured iron-based biocomposite: microstructure, degradation, and in vitro cell behavior. *Front Bioeng Biotechnol* 9:783821. <https://doi.org/10.3389/fbioe.2021.783821>
  89. Carluccio D, Bermingham M, Kent D, Demir AG, Previtali B, Dargusch MS (2019) Comparative study of pure iron manufactured by selective laser melting, laser metal deposition, and casting processes. *Adv Eng Mater* 21:7. <https://doi.org/10.1002/adem.201900049>
  90. Montani M, Demir AG, Mostaed E, Vedani M, Previtali B (2017) Processability of pure Zn and pure Fe by SLM for biodegradable metallic implant manufacturing. *Rapid Prototyp J* 23(3):514–523. <https://doi.org/10.1108/RPJ-08-2015-0100>
  91. Christof T, Steffen W, Julia R, Sobrero C, Sebastian D, Krooß P, Hans M, Thomas N (2021) On the microstructural and cyclic mechanical properties of pure iron processed by electron beam melting. *Adv Eng Mater* 23. <https://doi.org/10.1002/adem.202100018>
  92. Niendorf T et al (2015) Processing of new materials by additive manufacturing: iron-based alloys containing silver for biomedical applications. *Metall Mater Trans A Phys Metall Mater Sci* 46(7):2829–2833. <https://doi.org/10.1007/s11661-015-2932-2>
  93. Wackenrohr S et al (2022) Corrosion fatigue behavior of electron beam melted iron in simulated body fluid. *Npj Mater Degrad* 6:1. <https://doi.org/10.1038/s41529-022-00226-4>
  94. Rho J-Y, Kuhn-Spearing L, Zioupos P (1998) Mechanical properties and the hierarchical structure of bone. *Med Eng Phys* 20(2):92–102. [https://doi.org/10.1016/S1350-4533\(98\)00007-1](https://doi.org/10.1016/S1350-4533(98)00007-1)
  95. Al Mahmud MdZ, Mobarak MH, Hossain N, Islam MdA, Rayhan MdT (2023) Emerging breakthroughs in biomaterials for orthopedic applications: a comprehensive review. *Bioprinting* 36:e00323. <https://doi.org/10.1016/j.bprint.2023.e00323>
  96. Ma H et al (2021) PEEK (Polyether-ether-ketone) and its composite materials in orthopedic implantation. *Arab J Chem* 14(3):102977. <https://doi.org/10.1016/j.arabjc.2020.102977>
  97. Spierings AB, Herres N, Levy G (2011) Influence of the particle size distribution on surface quality and mechanical properties in AM steel parts. *Rapid Prototyp J* 17(3):195–202. <https://doi.org/10.1108/13552541111124770>
  98. Bekmurzayeva A, Duncanson WJ, Azevedo HS, Kanayeva D (2018) Surface modification of stainless steel for biomedical applications: revisiting a century-old material. *Mater Sci Eng, C* 93:1073–1089. <https://doi.org/10.1016/j.msec.2018.08.049>
  99. Xu W, Lui EW, Pateras A, Qian M, Brandt M (2017) In situ tailoring microstructure in additively manufactured Ti-6Al-4V for superior mechanical performance. *Acta Mater* 125:390–400. <https://doi.org/10.1016/j.actamat.2016.12.027>
  100. Leyens C, Manfred P (2003) Titanium and titanium alloys: fundamentals and applications. <https://doi.org/10.1002/3527602119>
  101. Acharya S, Soni R, Suwas S, Chatterjee K (2021) Additive manufacturing of Co–Cr alloys for biomedical applications: a concise review. *J Mater Res* 36(19):3746–3760. <https://doi.org/10.1557/s43578-021-00244-z>
  102. AlMangour B, Luqman M, Grzesiak D, Al-Harbi H, Ijaz F (2020) Effect of processing parameters on the microstructure and mechanical properties of Co–Cr–Mo alloy fabricated by selective laser melting. *Mater Sci Eng, A* 792:139456. <https://doi.org/10.1016/j.msea.2020.139456>
  103. Wauthle R et al (2015) Additively manufactured porous tantalum implants. *Acta Biomater* 14:217–225. <https://doi.org/10.1016/j.actbio.2014.12.003>
  104. Wang X, Ning B, Pei X (2021) Tantalum and its derivatives in orthopedic and dental implants: Osteogenesis and antibacterial properties. *Colloids Surf B Biointerfaces* 208:112055. <https://doi.org/10.1016/j.colsurfb.2021.112055>
  105. Massey CP, Havrilak CJ, Gussev MN, Terrani KA, Nelson AT (2021) Ultrasonic additive manufacturing of zirconium: pilot results. *Mater Lett* 302:130330. <https://doi.org/10.1016/j.matlet.2021.130330>
  106. Patil NA, Kandasubramanian B (2020) Biological and mechanical enhancement of zirconium dioxide for medical applications. *Ceram Int* 46(4):4041–4057. <https://doi.org/10.1016/j.ceramint.2019.10.220>
  107. Sui S et al (2023) Additive manufacturing of magnesium and its alloys: process-formability-microstructure-performance relationship and underlying mechanism. *Int J Extreme Manuf* 5(4):042009. <https://doi.org/10.1088/2631-7990/acf254>
  108. Properties and selection: nonferrous alloys and special-purpose materials. ASM International, 1990. <https://doi.org/10.31399/asm.hb.v02.9781627081627>
  109. Wen P et al (2018) Laser additive manufacturing of Zn metal parts for biodegradable applications: processing, formation quality and mechanical properties. *Mater Des* 155:36–45. <https://doi.org/10.1016/j.matdes.2018.05.057>
  110. Hernández-Escobar D, Champagne S, Yilmazer H, Dikici B, Boehlert CJ, Hermawan H (2019) Current status and perspectives of zinc-based absorbable alloys for biomedical applications. *Acta Biomater* 97:1–22. <https://doi.org/10.1016/j.actbio.2019.07.034>
  111. Kruth JP, Froyen L, Van Vaerenbergh J, Mercelis P, Rombouts M, Lauwers B (2004) Selective laser melting of iron-based powder. *J Mater Process Technol* 149(1–3):616–622. <https://doi.org/10.1016/j.jmatprotec.2003.11.051>
  112. Fan L, Chen S, Yang M, Liu Y, Liu J (2024) Metallic materials for bone repair. *Adv Healthc Mater* 13:3. <https://doi.org/10.1002/adhm.202302132>
  113. Gunasekaran J, Sevel P, John Solomon I (2021) Metallic materials fabrication by selective laser melting: a review. *Mater Today Proc* 37:252–256. <https://doi.org/10.1016/j.matpr.2020.05.162>
  114. Gruber H, Henriksson M, Hryha E, Nyborg L (2019) Effect of powder recycling in electron beam melting on the surface chemistry of alloy 718 powder. *Metall and Mater Trans A* 50(9):4410–4422. <https://doi.org/10.1007/s11661-019-05333-7>
  115. Gibson I, Rosen D, Stucker B, Khorasani M (2021) “Directed energy deposition,” in *Additive Manufacturing Technologies*, Cham: Springer International Publishing, 2021, pp. 285–318. [https://doi.org/10.1007/978-3-030-56127-7\\_10](https://doi.org/10.1007/978-3-030-56127-7_10)
  116. Mostafaei A et al (2021) Binder jet 3D printing—Process parameters, materials, properties, modeling, and challenges. *Prog Mater Sci* 119:100707. <https://doi.org/10.1016/j.pmatsci.2020.100707>
  117. ShrinivasMahale R et al (2022) Processes and applications of metal additive manufacturing. *Mater Today Proc* 54:228–233. <https://doi.org/10.1016/j.matpr.2021.08.298>

118. Gokuldoss PK, Sri K, Jürgen E (2017) Additive manufacturing processes: selective laser melting, electron beam melting and binder jetting—selection guidelines. *Materials* 10(6):672. <https://www.mdpi.com/1996-1944/10/6/672>
119. Lewin S, Fleps I, Åberg J, Ferguson SJ, Engqvist H, Öhman-Mägi C, Helgason B, Persson C (2021) Additively manufactured mesh-type titanium structures for cranial implants: E-PBF vs. L-PBF. *Mater Des* 197:109207. <https://doi.org/10.1016/j.matdes.2020.109207>
120. Béraud N, Vignat F, Villeneuve F, Dendievel R (2017) Improving dimensional accuracy in EBM using beam characterization and trajectory optimization. *Addit Manuf* 14:1–6. <https://doi.org/10.1016/j.addma.2016.12.002>
121. Willems N, Langenbach G, Everts V, Zentner A (2013) The microstructural and biomechanical development of the condylar bone: A review. *Eur J Orthod*:36. <https://doi.org/10.1093/ejo/cjt093>
122. Endo K, Yamada S, Todoh M, Takahata M, Iwasaki N, Tadano S (2016) Structural strength of cancellous specimens from bovine femur under cyclic compression. *PeerJ* 1:2016. <https://doi.org/10.7717/peerj.1562>
123. Wang X, Xu S, Zhou S, Xu W, Leary M, Choong P, Qian M, Brandt M, Xie YM (2016) Topological design and additive manufacturing of porous metals for bone scaffolds and orthopaedic implants: a review. *Biomaterials* 83:127–141. <https://doi.org/10.1016/j.biomaterials.2016.01.012>
124. Carnicero A, Peláez A, Restoy-Lozano A, Jacquot I, Perera R (2021) Improvement of an additively manufactured subperiosteal implant structure design by finite elements based topological optimization. *Sci Rep* 11:1. <https://doi.org/10.1038/s41598-021-94980-1>
125. Monkova K, Monka P, Zetkova I, Hanzl P, Mandulak D (2017) Three approaches to the gyroid structure modelling as a base of lightweight component produced by additive technology. In: *Proceedings of the 2nd international conference on computational modeling, simulation and applied mathematics (CMSAM 2017)*, Beijing. <https://dpi-journals.com/index.php/dtscse/article/view/16361>
126. Sychov MM, Lebedev LA, Dyachenko SV, Nefedova LA (2018) Mechanical properties of energy-absorbing structures with triply periodic minimal surface topology. *Acta Astronaut* 150:81–84. <https://doi.org/10.1016/j.actaastro.2017.12.034>
127. Melchels FPW, Bertoldi K, Gabbriellini R, Velders AH, Feijen J, Grijpma DW (2010) Mathematically defined tissue engineering scaffold architectures prepared by stereolithography. *Biomaterials* 31(27):6909–6916. <https://doi.org/10.1016/j.biomaterials.2010.05.068>
128. Yuan L, Ding S, Wen C (2018) Additive manufacturing technology for porous metal implant applications and triple minimal surface structures: a review. *Bioact Mater* 4:56–70. <https://doi.org/10.1016/j.bioactmat.2018.12.003>
129. Speirs M, Van Hooreweder B, Van Humbeeck J, Kruth JP (2017) Fatigue behaviour of NiTi shape memory alloy scaffolds produced by SLM, a unit cell design comparison. *J Mech Behav Biomed Mater* 70:53–59. <https://doi.org/10.1016/j.jmbbm.2017.01.016>
130. Yan C, Hao L, Hussein A, Young P (2015) Ti-6Al-4V triply periodic minimal surface structures for bone implants fabricated via selective laser melting. *J Mech Behav Biomed Mater* 51:61–73. <https://doi.org/10.1016/j.jmbbm.2015.06.024>
131. Javaid M, Haleem A (2018) Additive manufacturing applications in medical cases: a literature based review. *Alex J Med* 54(4):411–422. <https://doi.org/10.1016/j.ajme.2017.09.003>
132. Haleem A, Javaid M (2018) Role of CT and MRI in the design and development of orthopaedic model using additive manufacturing. *J Clin Orthop Trauma* 9(3):213–217. <https://doi.org/10.1016/j.jcot.2018.07.002>
133. Edelmann A, Dubis M, Hellmann R (2020) Selective laser melting of patient individualized osteosynthesis plates—digital to physical process chain. *Materials* 13(24):1–13. <https://doi.org/10.3390/ma13245786>
134. Plecko M et al (2012) Osseointegration and biocompatibility of different metal implants - a comparative experimental investigation in sheep. *BMC Musculoskelet Disord* 13:1. <https://doi.org/10.1186/1471-2474-13-32>
135. Cubillos PO, dos Santos VO, Pizzolatti ALA, Moré ADO, Roesler CRM (2022) Surface finish of total hip arthroplasty implants: are we evaluating and manufacturing them appropriately? *J Test Eval* 50:1. <https://doi.org/10.1520/JTE20200357>
136. Hayes JS, Geoff Richards R (2010) Surfaces to control tissue adhesion for osteosynthesis with metal implants: in vitro and in vivo studies to bring solutions to the patient. *Expert Rev Med Devices* 7(1):131–142. <https://doi.org/10.1586/erd.09.55>
137. Döbberthin C, Müller R, Meichsner G, Welzel F, Hackert-Oschätzchen M (2020) Experimental analysis of the shape accuracy in electrochemical polishing of femoral heads for hip endoprosthesis. *Procedia Manuf* 47:719–724. <https://doi.org/10.1016/j.promfg.2020.04.222>
138. Kourra N et al (2018) Computed tomography metrological examination of additive manufactured acetabular hip prosthesis cups. *Addit Manuf* 22:146–152. <https://doi.org/10.1016/j.addma.2018.04.033>
139. Zhao D et al (2022) Corrosion fatigue behavior and anti-fatigue mechanisms of an additively manufactured biodegradable zinc-magnesium gyroid scaffold. *Acta Biomater* 153:614–629. <https://doi.org/10.1016/j.actbio.2022.09.047>
140. Kaynak Y, Kitay O (2018) Porosity, surface quality, microhardness and microstructure of selective laser melted 316L stainless steel resulting from finish machining. *J Manuf Mater Proc* 2:2. <https://doi.org/10.3390/jmmp2020036>
141. “Review of surface finishing of additively manufactured metal implants,” 2020. [Online]. Available: <http://asmedigitalcollection.asme.org/MSEC/proceedings-pdf/MSEC2020/84256/V001T03A013/6619013/v001t03a013-msec2020-8419.pdf>
142. Teo A, Yan L, Chaudhari A, O’Neill G (2021) Post-processing and surface characterization of additively manufactured stainless steel 316L lattice: implications for BioMedical use. *Materials* 14. <https://doi.org/10.3390/ma14061376>
143. Maleki E, Bagherifard S, Bandini M, Guagliano M (2021) Surface post-treatments for metal additive manufacturing: Progress, challenges, and opportunities. *Addit Manuf* 37:101619. <https://doi.org/10.1016/j.addma.2020.101619>
144. Grzesiak D, Terelak-Tymczyna A, Bachtia-Radka E, Filipowicz K (2020) Technical and economic implications of the combination of machining and additive manufacturing in the production of metal parts on the example of a disc type element. In: Królczyk GM, Niesłony P, Królczyk J (eds) *Industrial measurements in machining*. Springer International Publishing, Cham, pp 128–137. [https://doi.org/10.1007/978-3-030-49910-5\\_12](https://doi.org/10.1007/978-3-030-49910-5_12)
145. Merola M, Affatato S (2019) Materials for hip prostheses: a review of wear and loading considerations. *Materials* 12:495. <https://doi.org/10.3390/ma12030495>
146. Syahrullail S, Sapawe N, Razak MD, Azli Y (2014) Effect of surface modification of acetabular cup with embedded micro-pits on friction properties. *Am J Mech Eng* 2(5):125–129. <https://doi.org/10.12691/ajme-2-5-1>
147. Safura HNL, Azli Y, Mohammed AK, Syahrullail S, Nazriah M (2012) Manufacturing methods for machining micro pits of hip implant for metal-on-metal lubrication. In: *2012 international*

- conference on biomedical engineering, ICoBE 2012. <https://doi.org/10.1109/ICoBE.2012.6178954>
148. Tej P, Karali P (2021) Micro-nano surface texturing, characterization and their impact on bio-interfaces. In: advanced machining and finishing. Elsevier Inc, pp 577–610. <https://doi.org/10.1016/B978-0-12-817452-4.00008-7>
  149. Lane JM, Jeffrey M, Aasis U, Hirsch BP, Shaffer AD, Shonuga OA (2011) Materials in fracture fixation. *Compr Biomater* 6:219–235. <https://doi.org/10.1016/B978-0-08-055294-1.00251-8>
  150. Huzum B et al (2021) Biocompatibility assessment of biomaterials used in orthopedic devices: an overview (review). *Exp Ther Med* 22:5. <https://doi.org/10.3892/etm.2021.10750>
  151. Frazier WE (2014) Metal additive manufacturing: a review. *J Mater Eng Perform* 23:1917–1928. <https://doi.org/10.1007/s11665-014-0958-z>
  152. Wu MW, Lai PH, Chen JK (2016) Anisotropy in the impact toughness of selective laser melted Ti-6Al-4V alloy. *Mater Sci Eng, A* 650:295–299. <https://doi.org/10.1016/j.msea.2015.10.045>
  153. Wang T, Zhu YY, Zhang SQ, Tang HB, Wang HM (2015) Grain morphology evolution behavior of titanium alloy components during laser melting deposition additive manufacturing. *J Alloys Compd* 632:505–513. <https://doi.org/10.1016/j.jallcom.2015.01.256>
  154. Sames W, Franziska L, Sreekanth P, Dehoff R, Sudarsanam B (2016) The metallurgy and processing science of metal additive manufacturing. *Int Mater Rev* 61:1–46. <https://doi.org/10.1080/09506608.2015.1116649>
  155. Wang X, Chou K “Residual stress in metal parts produced by powder-bed additive manufacturing processes,” 2015. [Online]. Available: <https://api.semanticscholar.org/CorpusID:44518071>
  156. Helmer H, Bauereiß A, Singer RF, Körner C (2016) Grain structure evolution in Inconel 718 during selective electron beam melting. *Mater Sci Eng, A* 668:180–187. <https://doi.org/10.1016/j.msea.2016.05.046>
  157. Kok Y et al (2018) Anisotropy and heterogeneity of microstructure and mechanical properties in metal additive manufacturing: a critical review. *Mater Des* 139:565–586. <https://doi.org/10.1016/j.matdes.2017.11.021>
  158. Ferrar B, Mullen L, Jones E, Stamp R, Sutcliffe CJ (2012) Gas flow effects on selective laser melting (SLM) manufacturing performance. *J Mater Process Technol* 212(2):355–364. <https://doi.org/10.1016/j.jmatprotec.2011.09.020>
  159. Wang X, Kevin C (2015) Residual stress in metal parts produced by powder-bed additive manufacturing processes. In: Proceedings of the 26th international solid freeform fabrication symposium, pp 1463–1474
  160. Parry L, Ashcroft IA, Wildman RD (2016) Understanding the effect of laser scan strategy on residual stress in selective laser melting through thermo-mechanical simulation. *Addit Manuf* 12:1–15. <https://doi.org/10.1016/j.addma.2016.05.014>
  161. Zhan Y, Xu H, Du W, Liu C (2022) Study on the effect of scanning strategy on residual stress in laser additive manufacturing with the laser ultrasound technique. *Exp Mech* 62(4):563–572. <https://doi.org/10.1007/s11340-021-00795-6>
  162. Shin W-S et al (2021) Heat treatment effect on the microstructure, mechanical properties, and wear behaviors of stainless steel 316L prepared via selective laser melting. *Mater Sci Eng, A* 806:140805. <https://doi.org/10.1016/j.msea.2021.140805>
  163. Wang S et al (2022) Role of porosity defects in metal 3D printing: formation mechanisms, impacts on properties and mitigation strategies. *Mater Today* 59:133–160. <https://doi.org/10.1016/j.mattod.2022.08.014>
  164. Friis EA, Tsao AK, Timmie Topoleski LD, Jones LC (2017) Introduction to mechanical testing of orthopedic implants. In: Friis E (ed) Mechanical testing of orthopaedic implants. Woodhead Publishing, pp 3–15. <https://doi.org/10.1016/B978-0-08-100286-5.00001-9>
  165. Jones LC, Timmie Topoleski LD, Tsao AK (2017) “Biomaterials in orthopaedic implants,” in Mechanical Testing of Orthopaedic Implants, Elsevier, 2017. <https://doi.org/10.1016/B978-0-08-100286-5.00002-0>
  166. Mohamed SR, Anwar S, Ghani C, Sawangsri W “Mechanical properties of additive manufactured CoCrMo meta- biomaterials for load bearing implants,” 2019. [Online]. Available: <https://api.semanticscholar.org/CorpusID:219325799>
  167. Lackey AD “Comparative study of mechanical properties of 316L stainless steel between traditional production methods and selective laser melting,” 2016. [Online]. Available: <https://api.semanticscholar.org/CorpusID:137895175>
  168. Azarniya A, Colera XG, Mirzaali MJ, Sovizi S, Bartolomeu F, St. Węglowski M, Wits WW, Yap CY, Ahn J, Miranda G, Silva FS, Hosseini HRM, Ramakrishna S, Zadpoor AA (2019) Additive manufacturing of Ti-6Al-4V parts through laser metal deposition (LMD): process, microstructure, and mechanical properties. *J Alloys Compd* 804:163–191. <https://doi.org/10.1016/j.jallcom.2019.04.255>
  169. Onal E, Frith JE, Jurg M, Wu X, Molotnikov A (2018) Mechanical properties and in vitro behavior of additively manufactured and functionally graded Ti6Al4V porous scaffolds. *Metals (Basel)* 8:4. <https://doi.org/10.3390/met8040200>
  170. Mohamed SR, Anwar S, Ghani C, Sawangsri W (2019) Mechanical properties of additive manufactured CoCrMo meta- biomaterials for load bearing implants. <https://api.semanticscholar.org/CorpusID:219325799>
  171. Mergulhão MV, Das Neves MDM (2018) Characteristics of biometallic alloy to additive manufacturing using selective laser melting technology. *J Biomater Nanobiotechnol* 09(01):89–99. <https://doi.org/10.4236/jbnb.2018.91008>
  172. Lackey AD (2016) Comparative study of mechanical properties of 316L stainless steel between traditional production methods and selective laser melting. North Carolina University System. <https://ui.adsabs.harvard.edu/abs/2016PhDT.....37L>
  173. Meenashisundaram GK, Xu Z, Nai MLS, Lu S, Ten JS, Wei J (2020) Binder jetting additive manufacturing of high porosity 316L stainless steel metal foams. *Materials* 13:17. <https://doi.org/10.3390/MA13173744>
  174. Qiong W, Eltit F, Wang R (2017) Corrosion of orthopedic implants. In: Reference module in biomedical sciences. <https://doi.org/10.1016/B978-0-12-801238-3.99863-5>
  175. Mah D, Pelletier MH, Lovric V, Walsh WR (2019) Corrosion of 3D-printed orthopaedic implant materials. *Ann Biomed Eng* 47(1):162–173. <https://doi.org/10.1007/s10439-018-02111-1>
  176. Gai X, Bai Y, Li S, Wang L, Ai S, Hao YL, Yang R, Dai K (2021) Review on corrosion characteristics of porous titanium alloys fabricated by additive manufacturing. *J Shanghai Jiaotong Univ (Science)* 26:416–430. <https://doi.org/10.1007/s12204-021-2314-4>
  177. Li J, Qin L, Yang K, Ma Z, Wang Y, Cheng L, Zhao D (2020) Materials evolution of bone plates for internal fixation of bone fractures: a review. *J Mater Sci Technol* 36:190–208. <https://doi.org/10.1016/j.jmst.2019.07.024>
  178. Mandal S, Ummadi R, Bose M, Balla VK, Roy M (2019) Fe–Mn–Cu alloy as biodegradable material with enhanced antimicrobial properties. *Mater Lett* 237:323–327. <https://doi.org/10.1016/j.matlet.2018.11.117>
  179. Weiss L, Nessler Y, Novelli M, Laheurte P, Grosdidier T (2019) On the use of functionally graded materials to differentiate the effects of surface severe plastic deformation, roughness and

- chemical composition on cell proliferation. *Metals* (Basel) 9:12. <https://doi.org/10.3390/met9121344>
180. Al-Mamun NS, Mairaj Deen K, Haider W, Asselin E, Shabib I (2020) “Corrosion behavior and biocompatibility of additively manufactured 316L stainless steel in a physiological environment: the effect of citrate ions.” *Addit Manuf*, 34 <https://doi.org/10.1016/j.addma.2020.101237>
  181. Park JY, Davies JE (2000) Red blood cell and platelet interactions with titanium implant surfaces. *Clin Oral Implants Res* 11(6):530–539. <https://doi.org/10.1034/j.1600-0501.2000.011006530.x>
  182. Santamaria M, Tranchida G, Di Franco F (2020) Corrosion resistance of passive films on different stainless steel grades in food and beverage industry. *Corros Sci* 173:108778. <https://doi.org/10.1016/j.corsci.2020.108778>
  183. Bernhardt A, Schneider J, Schroeder A, Papadopoulos K, Lopez E, Brückner F, Botzenhart U (2021) Surface conditioning of additively manufactured titanium implants and its influence on materials properties and in vitro biocompatibility. *Mater Sci Eng: C* 119:111631. <https://doi.org/10.1016/j.msec.2020.111631>
  184. Qin Y et al (2022) Processing optimization, mechanical properties, corrosion behavior and cytocompatibility of additively manufactured Zn-0.7Li biodegradable metals. *Acta Biomater* 142:388–401. <https://doi.org/10.1016/j.actbio.2022.01.049>
  185. Spratt M, Newkirk J, Chandrashekhara K (2016) Fabrication of metal matrix syntactic foams by a laser additive manufacturing process. <https://api.semanticscholar.org/CorpusID:136336864>
  186. Cagirici M, Wang P, Ng FL, Nai MLS, Ding J, Wei J (2021) Additive manufacturing of high-entropy alloys by thermophysical calculations and in situ alloying. *J Mater Sci Technol* 94:53–66. <https://doi.org/10.1016/j.jmst.2021.03.038>
  187. Wang SP, Xu J (2017) TiZrNbTaMo high-entropy alloy designed for orthopedic implants: As-cast microstructure and mechanical properties. *Mater Sci Eng, C* 73:80–89. <https://doi.org/10.1016/j.msec.2016.12.057>
  188. Cai C et al (2019) In-situ preparation and formation of TiB/Ti-6Al-4V nanocomposite via laser additive manufacturing: microstructure evolution and tribological behavior. *Powder Technol* 342:73–84. <https://doi.org/10.1016/j.powtec.2018.09.088>
  189. Zhang C, Ouyang D, Pauly S, Liu L (2021) 3D printing of bulk metallic glasses. *Mater Sci Eng R: Rep* 145:100625
  190. Afolabi LO, Ariff ZM, Hashim SFS, Alomayri T, Mahzan S, Kamarudin KA, Muhammad ID (2020) Syntactic foams formulations, production techniques, and industry applications: a review. *J Mater Res Technol* 9:10698–10718. <https://api.semanticscholar.org/CorpusID:225318700>
  191. Kumar S, Raj S, Jain S, Chatterjee K (2016) Multifunctional biodegradable polymer nanocomposite incorporating graphene-silver hybrid for biomedical applications. *Mater Des* 108:319–332. <https://doi.org/10.1016/j.matdes.2016.06.107>
  192. Smith SE et al (2017) Homogenized porcine extracellular matrix derived injectable tissue construct with gold nanoparticles for musculoskeletal tissue engineering applications. *J Biomater Nanobiotechnol* 08(02):125–143. <https://doi.org/10.4236/jbnb.2017.82009>
  193. Po-Yuan Y, Jacob H, Jason J, Cheng-Tang P, Chung-Hwan C, Che-Hsin L (2022) Recent developments in additive-manufactured intermetallic compounds for bio-implant applications. *J Med Biol Eng* 42. <https://doi.org/10.1007/s40846-022-00753-0>
  194. Torralba JM, Campos M (2020) High entropy alloys manufactured by additive manufacturing. *Metals* (Basel) 10:5. <https://doi.org/10.3390/met10050639>
  195. Sohrabi N, Jhabvala J, Logé R (2021) Additive manufacturing of bulk metallic glasses—process, challenges and properties: a review. *Metals* 11:1279. <https://doi.org/10.3390/met11081279>
  196. Singh AK, Patil B, Hoffmann N, Saltonstall B, Doddamani M, Gupta N (2018) Additive manufacturing of syntactic foams: Part I: development, properties, and recycling potential of filaments. *JOM* 70(3):303–309. <https://doi.org/10.1007/s11837-017-2734-7>
  197. Hou C, Liu Y, Wei X, Xin L, Guo L, Liu Y, Tian S, Liu B, Zhang J, Wen C (2022) Additive manufacturing of functionally graded porous titanium scaffolds for dental applications. *Biomater Adv* 139:213018. <https://doi.org/10.1016/j.bioadv.2022.213018>
  198. Adam B, Aleksandra B, Daria F, Zuzanna G, Dawid T, Kinga K, Robert K, Marcin M, Jacek B (2023) Application of 3D printing in bone grafts. *Cells* 12(6):859. <https://www.mdpi.com/2073-4409/12/6/859>
  199. Chacón JM, Núñez PJ, Caminero MA, García-Plaza E, Vallejo J, Blanco M (2022) 3D printing of patient-specific 316L–stainless-steel medical implants using fused filament fabrication technology: two veterinary case studies. *Biodes Manuf* 5(4):808–815. <https://doi.org/10.1007/s42242-022-00200-8>
  200. Liu J, Rafiq M, Bte N, Wong LM, Wang S (2021) Surface treatment and bioinspired coating for 3D-printed implants. *Front Chem* 9:768007. <https://doi.org/10.3389/fchem.2021.768007>
  201. Dwivedi S, Dixit AR, Das AK, Adamczuk K (2022) Additive texturing of metallic implant surfaces for improved wetting and biotribological performance. *J Market Res* 20:2650–2667. <https://doi.org/10.1016/j.jmrt.2022.08.029>

**Publisher's Note** Springer Nature remains neutral with regard to jurisdictional claims in published maps and institutional affiliations.